KTH Engineering Sciences

Simulations of thermoelectric transport in granular superconductors

ANDREAS ANDERSSON

Licentiate thesis
Stockholm, Sweden 2010

TRITA 2010:27
ISSN 0280-316X
ISRN KTH/FYS/2010:27-SE
ISBN 978-91-7415-659-1

KTH Teoretisk fysik
AlbaNova universitetscentrum
SE-106 91 Stockholm Sweden

Akademisk avhandling som med tillstånd av Kungl Tekniska högskolan framlägges till offentlig granskning för avläggande av teknologie licentiatexamen i teoretisk fysik den 9 juni 2010 kl 10:00 i sal FD51, AlbaNova Universitetscentrum.

Tryck: Universitetsservice US AB

Abstract

This thesis presents results from numerical simulations of the Nernst effect due to phase fluctuations in models of two-dimensional granular superconductors. In addition other transport properties, such as thermal conductivity and electrical resistivity are calculated. The models are based on a phase only description with Langevin or resistively and capacitively shunted Josephson junction (RCSJ) dynamics, generalized to be valid for any type of two-dimensional lattice structure. All transport coefficients are evaluated from equilibrium correlation functions using Kubo formulas.

In Paper I, anomalous sign reversals of the Nernst signal e_N, corresponding to vortex motion from colder to hotter regions, are observed. These are attributed to geometric frustration effects close to magnetic fields commensurate with the underlying lattice structure. The effect is seen also in systems with moderate geometric disorder, and should thus be possible to observe in real two-dimensional granular superconductors or Josephson junction arrays.

Paper II presents two different derivations of an expression for the heat current in Langevin and RCSJ dynamics. The resulting expression is through our simulations seen to obey the required Onsager relation, as well as giving consistent results when calculating κ and e_N via Kubo formulas and through the responses to an applied temperature gradient. In zero magnetic field and at low-temperatures, the contribution to the thermal conductivity κ in RCSJ dynamics is calculated using a spin-wave approximation, and is shown to be independent of temperature and diverge logarithmically with system size. At higher temperatures, κ shows a non-monotonic temperature dependence. In zero magnetic field κ has a anomalous logarithmic size dependence also in this regime. The off-diagonal component of the thermoelectric tensor α_{xy} is calculated and displays the very same $\sim 1/T$ dependence at low temperatures predicted from calculations based on Gaussian superconducting fluctuations.

Preface

The thesis you now hold in your hands represents my academic deed so far. It summarizes the work I have done as a PhD student at the KTH Department of Theoretical Physics from spring 2007 to spring 2010. The thesis is divided into two parts. The first part gives some background to the topics covered in the papers, as well as details regarding the models and simulation methods used and a summary of the important results. The second part consists of the papers listed below.

List of papers

Paper I. Anomalous Nernst effect and heat transport by vortex vacancies in granular superconductors, Andreas Andersson and Jack Lidmar,
Physical Review B 81, 060508(R) (2010) [1].

Paper II. Heat transport and thermoelectric effects in granular superconductors, Andreas Andersson and Jack Lidmar, *Preprint* [2].

Comments on my contributions to the papers

Paper I.
The topic was suggested to me by Dr. Lidmar. I wrote all the simulation code, produced the figures and co-wrote the paper.

Paper II.
A large part of the analytical calculations in this paper was done by Dr. Lidmar. I did parts of the calculations, wrote all the simulation code, produced the figures and co-wrote the paper.

Acknowledgments

I would first of all like to deeply thank my main supervisor Associate Professor Jack Lidmar for his most invaluable guidance, encouragement and kind ways in the venture leading to this thesis. I also send my warmest gratitudes towards Professor Mats Wallin, for letting me join the Statistical Physics group as a PhD student.

During the my years at this department I have stayed in the same great room, with an ever-changing crowd of Master thesis and PhD students. You are all remembered, especially my long-term room mates, in order of disappearance, Marios Nikolaou, Martin Lindén and Anders Biltmo. A big thanks also to my present roomie Hannes Meier, my source to classical music I didn't know I liked and South Park epsiodes I didn't know existed. It's a pleasure sharing office space with you! At coffee and lunch breaks I have very much enjoyed the conversations with my other fellow PhD students Erik Brandt, Richard Tjörnhammar and Johan Carlström. Erik, my good old friend during our long common path at KTH, I wish you the best of luck and hope you'll continue your Kramer-esque appearances in our room!

Lastly, I'm indebted to all parts of my big family, the Anderssons, the Archentis, the Ernevings and the Bratels for their care and support, even though I've often struggled to explain what exactly I've been up to these past couple of years.

Above all I thank Yaël, my true love, for believing in me at times when I don't, and for making my life so much brighter.

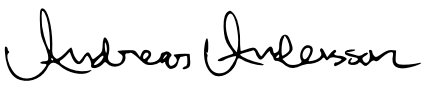

Andreas Andersson,
Stockholm, May 12, 2010.

Contents

Part I

Background

Chapter 1

Introduction and thesis outline

The Nernst effect can in a sense be viewed as the thermal equivalent to the well known classical Hall effect. In both effects an electric field is induced in presence of a perpendicular magnetic field, but while for the Hall effect the driving force is an electric current, the Nernst effect arises due to an applied temperature gradient.

The effect in normal metals is a quite a dated discovery, made in the late nineteenth century by the German scientist Walther Hermann Nernst, who later became the 1920 Nobel laureate in chemistry. In superconductors, the first experimental measurements of the Nernst effect where performed in the late 1960s. The effect was then measured in the mixed state of type-II superconductors [3, 4] as well as in the intermediate state of type-I superconductors [5], and was attributed to the flow of thermally driven vortices. Also numerous later experiments on high-T_c cuprate superconductors done in the 90s [6, 7, 8] used the vortex explanation, adopting a phenomenological theory (introduced in the 1960s experimental papers) in their analysis, where vortices are subject to a thermal force in presence of a temperature gradient, due to their finite entropy.

At the turn of the century the field gained new momentum when Ong's group made complementary measurements on cuprates at higher magnetic field strengths, finding a sizable Nernst signal well above T_c in the disputed pseudogap phase [9, 10, 11, 12]. They concluded that the signal was of vortex origin and interpreted this as evidence for vortex excitations in the pseudogap. These findings sparked a number of theoretical investigations regarding the origin of the large Nernst effect in cuprates. In the first of these papers, Ussishkin *et al.* [13] calculated the contribution to the Nernst effect from fluctuations of the amplitude of the superconducting order parameter using time-dependent Ginzburg-Landau theory within a Gaussian approximation. They found quantitative agreement with the Nernst effect in the hole doped cuprate $La_{2-x}Sr_xCuO_4$ at low magnetic fields close to T_c. A simulation paper by Mukerjee and Huse [14] using the same time-dependent Ginzburg-Landau dynamics found reasonable agreement with data from $La_{2-x}Sr_xCuO_4$ as well as another hole doped cuprate $Bi_2Sr_2CaCu_2O_{8+x}$, also in the high magnetic field limit.

The scenario of amplitude fluctuations of the superconducting order parameter (also called Cooper pair fluctuations in the literature) as a source of the Nernst effect in superconductors, where later supported also by experiments on conventional thin film superconductors [15, 16] and by more recent theory papers [17, 18] examining the problem using a microscopic approach. The effect of phase fluctuations of the superconducting order parameter (i.e. vortices) on the Nernst effect was studied in a paper by Podolsky *et al.* [19] a few years ago. They simulated a two-dimensional phase only model with model-A dynamics, essentially equivalent to the Langevin model we use in Paper I (apart from boundary conditions and a few other simulation-technical details) and find some agreement with experimental findings in $La_{2-x}Sr_xCuO_4$. Other proposed explanations to the large Nernst effect above the transition temperature in high-T_c superconductors include proximity to a quantum critical point [20] and enhancement of the Nernst signal from stripe order in an experimental paper published in Nature last year by Cyr-Choiniere *et al.* (followed by a theoretical investigation backing up this scenario [21]). The latter view was however challenged very recently in a publication presenting new measurements on cuprates made by Ong's group [22].

This thesis focuses its attention to the Nernst effect due to phase fluctuations in two-dimensional superconducting systems. The models we construct are primarily applicable to granular systems, not necessarily of high-T_c type, but can under certain conditions also be valid for continuous thin-film superconductors or even highly anisotropic quasi-two-dimensional bulk superconductors, such as some of the cuprates mentioned above. In addition to the Nernst effect, some interesting aspects of the closely related thermal conductivity will also be investigated within the framework of our models.

The outline of the thesis is as follows. In Chapter 2 an introduction to some important models and concepts in superconductivity and non-equilibrium thermodynamics related to our work will be given. Chapter 3 discusses mainly Langevin, RSJ and RCSJ dynamics and how these are implemented in our simulations. Chapter 4 presents a summary of the results of our numerical and analytical calculations, and is intended as an introduction to Paper I and II. Finally, the concluding Chapter 5 is a brief summary of the thesis.

Chapter 2

Theory background

This chapter is an introduction to theoretical concepts and models, needed to fully appreciate the rest of this thesis.

2.1 Ginzburg-Landau theory of superconductivity

Even before a solid understanding of the microscopic mechanisms behind superconductivity was reached with the theory of Bardeen, Cooper and Schrieffer (BCS) in their 1957 paper [23], a theory existed that could describe the nature of the superconducting state on phenomenological level. This was the theory of Ginzburg and Landau (GL) [24]. It has been used ever since, with great success due to its powerful simplicity, to explain superconducting phenomena. The theory is based on Landau's general theory of second-order phase transitions that introduces the concept of an order parameter, which is non-zero below the transition point and vanishes above it. In the GL theory, the order parameter is the complex superconducting wave function Ψ, which can be written as

$$\Psi(\mathbf{r}) = |\Psi(\mathbf{r})|e^{i\theta(\mathbf{r})} = \sqrt{n(\mathbf{r})}e^{i\theta(\mathbf{r})}, \tag{2.1}$$

where $n(\mathbf{r})$ is the density of Cooper pairs. If we assume that Ψ is small close to the transition temperature and changes slowly in space the total free energy of the superconductor can be expressed as an expansion in the order parameter and its gradients. From general symmetry considerations [25] one can show that the expansion only can include terms of even powers. The result is the GL free energy functional

$$F_{GL}[\Psi(\mathbf{r})] = F_N + \int \mathrm{d}^d r \left[\alpha|\Psi(\mathbf{r})|^2 + \frac{\beta}{2}|\Psi(\mathbf{r})|^4 + \frac{1}{2m}|(\frac{\hbar}{i}\nabla - q\mathbf{A})\Psi(\mathbf{r})|^2 + \frac{\mathbf{B}^2}{2\mu_0} \right], \tag{2.2}$$

where $\mathbf{B} = \nabla \times \mathbf{A}$ is the applied magnetic field and F_N the free energy of the normal state.

Landau's theory of phase transitions tells us that the coefficient $\alpha(T)$ to lowest order around T_c has the form $\alpha(T) = \alpha_0(T - T_c)$ (where $\alpha_0 > 0$), so that it is positive above T_c and changes sign at the phase transition. Further $\beta > 0$, since would it be negative, the free energy could be made arbitrarily small (negative and large) by making Ψ large, a situation for which the free energy expansion above is obviously not applicable. Note also that the coefficient in front of the gradient term is generally positive in Landau theory. Here it can be fixed by remembering that in quantum mechanics the gauge invariant form of mass times velocity for a particle of charge q and mass m is

$$m\mathbf{v} = \frac{\hbar}{i}\nabla - q\mathbf{A}. \tag{2.3}$$

From this we see that the gradient term in (2.2) is nothing but the kinetic energy $m\mathbf{v}^2/2$ of a particle with mass m, if the coefficient is set to $1/2m$.

By minimizing the GL free energy (2.2), with respect to variations in Ψ we get the first GL equation

$$\alpha\Psi + \beta|\Psi|^2\Psi + \frac{1}{2m}(\frac{\hbar}{i}\nabla - q\mathbf{A})^2\Psi = 0 \tag{2.4}$$

Doing the same with respect to variations in the vector potential $\mathbf{A}$ together with Ampére's law, relating the current density $\mathbf{J}$ to the curl of the magnetic field $\mathbf{B}$, $\mu_0\mathbf{J} = \nabla \times \mathbf{B}$, yields the second GL equation

$$\mathbf{J} = \frac{q}{2m}(\Psi^*(\frac{\hbar}{i}\nabla - q\mathbf{A})\Psi + \Psi(-\frac{\hbar}{i}\nabla - q\mathbf{A})\Psi^*), \tag{2.5}$$

or equivalently by rewriting Ψ in a polar form given by (2.1)

$$\mathbf{J} = \frac{q}{m}|\Psi(\mathbf{r})|^2(\hbar\nabla\theta(\mathbf{r}) - q\mathbf{A}). \tag{2.6}$$

The expression for the supercurrent above is exactly that found from quantum mechanics for particles with effective charge and mass q and m respectively, in presence of a magnetic field $\mathbf{B} = \nabla \times \mathbf{A}$ (not surprising since we fixed the coefficient above to do precisely this). At the time of birth of the GL theory (1950), the phenomenon of Cooper pairing was not known, and therefore Landau and Ginzburg identified q with the charge of an electron $-e$. The correct form of the GL free energy with $q = -2e$ was established by Gor'kov in 1959 [26] as he showed that the GL theory can be derived from the microscopic BCS theory.

Now look at the first GL equation (2.4) above. Since each term in that expression must be of the same dimensionality, we know for example that $\alpha\Psi$ and $\frac{\hbar^2}{2m}\nabla\Psi$ (the gradient part of the kinetic term) have the same dimension. This implies the existence of a characteristic length ξ, relating the coefficients of the two terms so that $\frac{\hbar^2}{2m} = |\alpha|\xi^2$ (where $\alpha = -|\alpha|$ below T_c). This quantity is the correlation length

or coherence length, and can be written as

$$\xi = \sqrt{\frac{\hbar^2}{2m|\alpha|}}. \tag{2.7}$$

The coherence length sets the length scale of the fluctuations of the order parameter field Ψ in the model. Note that at $T = T_c$ the coefficient α goes to zero and ξ diverges, a general property of second order phase transitions.

The length scale on which fluctuations of the magnetic vector potential $\mathbf{A}$ occur in the GL theory is set by the so called penetration length (or penetration depth) λ. This length can be derived by a similar dimensionality analysis as above. Combining the second GL equation (2.6) with Ampére's law yields

$$\nabla \times \mathbf{B} = \nabla \times (\nabla \times \mathbf{A}) = \mu_0 \mathbf{J} = \mu_0 \frac{q}{m} |\Psi(\mathbf{r})|^2 (\hbar \nabla \theta(\mathbf{r}) - q\mathbf{A}). \tag{2.8}$$

This equation tells us that $\nabla \times \nabla \times \mathbf{A}$ has the same dimension as $(\mu_0 q^2 |\Psi|^2/m)\mathbf{A}$, i.e., there is a length λ such that $\mu_0 q^2 |\Psi|^2/m = 1/\lambda^2$, giving us the final expression for the penetration length

$$\lambda = \sqrt{\frac{m}{\mu_0 q^2 |\Psi|^2}}. \tag{2.9}$$

Taking the ratio of these two lengths ξ and λ gives the Ginzburg-Landau parameter

$$\kappa = \lambda/\xi, \tag{2.10}$$

which is the only free parameter needed to describe a superconductor within the GL theory [27].

2.2 Vortices

As a superconducting material is placed in a weak magnetic field $\mathbf{H}$, the superconductor will expel the field, or more precisely, $\mathbf{B} = 0$ inside the material except from a thin boundary layer of typical depth λ, where the field is exponentially decaying and screening supercurrents flow to set up a field that exactly cancels the field inside the sample. This is the well known Meissner effect.

When increasing the magnetic field, there are two very different scenarios depending on the size of the GL parameter κ, defined above. For materials with small values of κ, a category in which most ordinary pure metals fall, the magnetic field will penetrate the entire sample and destroy superconductivity at and above $\mathbf{H} = \mathbf{H_c}$, the upper critical field. These materials are termed type-I superconductors. Materials with large κ, such as certain metals, metal alloys and ceramic high temperature (high-T_c) superconductors, are called type-II. The difference between them lies in the nature of the phase transition in a magnetic field due to the fact that the surface energy of the interface between the superconducting and normal

phase have different signs for the two types (the sign change happens at precisely $\kappa = 1/\sqrt{2}$, shown numerically by Ginzburg and Landau in their original 1950 paper [24]). In type-II superconductors the surface energy is negative and it can thus be energetically favorable to have mix of the two phases, since an increase of the free energy due to the introduction of a normal region in the superconducting phase could be compensated by the negative free energy contribution of the interface. This mixed phase is present at fields $\mathbf{H_{c1}} < \mathbf{H} < \mathbf{H_{c2}}$. The normal regions where the magnetic flux passes through the sample are called vortex lines or just vortices. The flux carried by a vortex is quantized, which can be seen by studying the second GL equation (2.6). If we think of an integration path going around far away from the vortex inside the superconductor, where there is no magnetic field $\mathbf{B}$ and thus no supercurrent, $\mathbf{J} = 0$, we have from (2.6)

$$\oint \frac{\hbar}{2e} \nabla\theta(\mathbf{r}) \cdot d\mathbf{r} = \oint \mathbf{A} \cdot d\mathbf{r}. \tag{2.11}$$

The right hand side can be transformed to a surface integral using Stokes' theorem

$$\oint \mathbf{A} \cdot d\mathbf{r} = \int (\nabla \times \mathbf{A}) \cdot d\mathbf{S} = \int \mathbf{B} \cdot d\mathbf{S} = \Phi, \tag{2.12}$$

and we see that this integral represents simply the flux Φ through the integrated surface, which is the same as the flux carried by the vortex. The left hand side amounts to just the difference in the phase θ making the closed loop integration. Since the order parameter Ψ must be single valued, this difference should be a multiple of 2π

$$\oint \nabla\theta(\mathbf{r}) \cdot d\mathbf{r} = 2\pi n, \tag{2.13}$$

with n an integer. This leads to the following quantization condition for the flux Φ carried by a vortex

$$\Phi = n\frac{h}{2e} \equiv n\Phi_0, \tag{2.14}$$

where $\Phi_0 = h/2e$ is the flux quantum.

Vortex lattice

In a defect free type-II superconductor Abrikosov [28] showed that vortices in the mixed state will form a regular triangular lattice (actually he made a numerical error in his original paper which led him to conclude that a square array had the lowest energy, but this was later corrected by Kleiner, Roth and Autler [29]). This description is true for conventional superconducting materials, but in the case of high-temperature superconductors the enhanced effects of thermal fluctuations might melt the lattice into a vortex liquid. By the introduction of random defects in the material there is also the possibility of different types vortex-glass phases [30, 31].

Vortex motion

So what happens when vortices move, for example in the vortex liquid phase? On a phenomenological level one can make the following analysis. Running an external current density $\mathbf{J}$ through a superconductor, will make a perpendicular Lorentz force $\mathbf{F_L} = \mathbf{J} \times \hat{\mathbf{b}}\Phi_0$ act on a unit length of every vortex line in the sample ($\hat{\mathbf{b}}$ is a unit vector in the direction of the magnetic field). In a homogeneous defect free superconductor the vortices will start to move in response to this force (in the Abrikosov vortex lattice phase the entire vortex lattice can start to move rigidly) and feel a friction force $\mathbf{F_f} = -\eta\mathbf{v}$ per unit length of the vortex line, where η is the damping viscosity of the vortex fluid (measured in N·s/m^2). In steady state these two forces balance each other so that $\mathbf{F_L} + \mathbf{F_f} = 0$, which then gives a vortex velocity $\mathbf{v_v} = \mathbf{J} \times \hat{\mathbf{b}}\Phi_0/\eta$ perpendicular to the applied current and magnetic field. According to Faraday's law, the flow of the magnetic flux penetrating the vortices causes the generation of an electric field transverse to their motion [32]

$$\mathbf{E} = -\mathbf{v_v} \times \mathbf{B}. \tag{2.15}$$

Notice that $\mathbf{E}$ has a component parallel to the applied current density $\mathbf{J}$ leading to a power dissipation per unit volume of $\mathbf{E} \cdot \mathbf{J}$, which can be detected as a finite linear resistivity (a so called flux flow resistivity) in the direction of $\mathbf{J}$ given by

$$\rho_f = \mathbf{E} \cdot \mathbf{J}/J^2 = B\Phi_0/\eta, \tag{2.16}$$

assuming $\mathbf{E} \parallel \mathbf{J}$. This leads us to the conclusion that moving vortices cause dissipation and therefore true superconductivity is not possible in perfectly homogeneous type-II superconductors. In real superconductors, however, the ever present defects will (at least at low temperatures) pin the vortices, making them immobile in the case of a weak applied current (weak enough so that the pinning force can match the Lorentz force), restoring the superconductivity hallmark of zero resistance.

Vortices in 2D - the Berezinskii-Kosterlitz-Thouless transition

There is an essential difference between vortices in two and three dimensions. As we have seen previously, vortices in 3D superconductors appear when a high enough magnetic field is applied. However, in 2D vortices can also be induced by thermal fluctuations. As shown in the works by Berezinskii [33] and Kosterlitz and Thouless [34], in two dimensions thermally induced vortices and antivortices exist in bound pairs in the low temperature phase, but as the temperature is raised above a certain temperature T_{BKT} the pairs unbind (in zero magnetic field the densities of vortices and antivortices are equal). The motion of these free vortices will as consequence induce an electric field, which leads to dissipation and the loss of true superconductivity as explained in the previous section. The Berezinskii-Kosterlitz-Thouless transition can take place both 2D systems such as superconducting thin-films and 2D Josephson junction arrays, as well as in highly anisotropic bulk superconductors with quasi-two-dimensional structure, e.g., the cuprate BiSrCaCuO.

2.3 Tunnel junctions and Josephson effects

A tunnel junction is a system where two superconductors are joined together by some kind weak link, i.e., a region where superconductivity is somehow suppressed. A weak link can be realized in several ways. The most common cases are those where two superconductors are separated by a thin insulating or a normal metal layer. These junctions are referred to as SIS and SNS junctions respectively. Another type is the ScS junction, where c stands for some type of constriction, for example a region with significantly reduced cross-sectional area. The interest in these systems began in 1962 with the work of Josephson [35], who predicted that two weakly coupled superconductors would have new and unexpected properties. What follows is a derivation due to Feynman [36] of the two governing equations Josephson found and which bare his name.

We consider a model of a one-dimensional Josephson junction, as a system of two superconductors separated by an insulating layer, acting as a potential barrier for the Cooper pairs. If the layer is thin enough the tunneling amplitude of the electron pairs is finite and the two superconductors are weakly coupled. Let the wave function of the Cooper pairs on one side be denoted by Ψ_1 and on the other side by Ψ_2. Assume also for simplicity that there is no magnetic field present. The equations of motion for the probability amplitudes are then simply

$$i\hbar\frac{\partial\Psi_1}{\partial t} = E_1\Psi_1 + K\Psi_2, \quad i\hbar\frac{\partial\Psi_2}{\partial t} = E_2\Psi_2 + K\Psi_1, \tag{2.17}$$

i.e., two coupled Schrödinger equations, where K is a coupling parameter, which depends on the nature of the insulating barrier. Suppose that we connect the system to a battery, so that a constant potential difference $E_1 - E_2 = 2eV$ is kept across the junction. By further defining the zero of energy at $(E_1 + E_2)/2$, we get

$$i\hbar\frac{\partial\Psi_1}{\partial t} = \frac{eV}{2}\Psi_1 + K\Psi_2, \quad i\hbar\frac{\partial\Psi_2}{\partial t} = -\frac{eV}{2}\Psi_2 + K\Psi_1. \tag{2.18}$$

Now rewrite these equations using a polar representation of the generally complex probability amplitudes Ψ_1 and Ψ_2

$$\Psi_1 = \sqrt{n_1}e^{i\theta_1}, \quad \Psi_2 = \sqrt{n_2}e^{i\theta_2}, \tag{2.19}$$

and equate real and imaginary parts separately to obtain

$$\dot{n}_1 = \frac{2K}{\hbar}\sqrt{n_1 n_2}\sin(\theta_2 - \theta_1), \qquad \dot{n}_2 = -\frac{2K}{\hbar}\sqrt{n_1 n_2}\sin(\theta_2 - \theta_1)$$
$$\dot{\theta}_1 = \frac{K}{\hbar}\sqrt{\frac{n_2}{n_1}}\cos(\theta_2 - \theta_1) - \frac{eV}{\hbar}, \qquad \dot{\theta}_2 = \frac{K}{\hbar}\sqrt{\frac{n_1}{n_2}}\cos(\theta_2 - \theta_1) + \frac{eV}{\hbar}.$$

The current I from side 1 to 2 is just given by $2e\dot{n}_1$ (or $-2e\dot{n}_2$), so the first pair of equations tells us that

$$I = I_c\sin(\theta_2 - \theta_1), \tag{2.20}$$

where $I_c = \frac{4eK}{\hbar}\sqrt{n_1 n_2}$ is the critical current of the junction, which is the maximum current the junction can carry. We call the equation above the first or DC Josephson equation. It states that the tunneling supercurrent through the junction depends only on the phase difference between the two sides. Taking the difference of the two remaining equations assuming the superconducting material on both sides of the junction is the same, $n_1 = n_2$, gives the second Josephson equation

$$\dot{\theta}_2 - \dot{\theta}_1 = \frac{2e}{\hbar}V. \tag{2.21}$$

Combining the first and the second Josephson equation, it is easy to see that the presence of a voltage V across the junction, will generate an oscillating supercurrent with frequency $\omega = 2eV/\hbar$. This is the AC Josephson effect. The previous relation provides a link between frequency and voltage and has actually been used to define the standard volt. Josephson junctions are today used in many types of sophisticated electronic equipment, mainly as very sensitive magnetometers, so called SQUID:s.

Remember, however, that the above derivation is true only for the case of no magnetic field. In a magnetic field the phase difference $\theta_2 - \theta_1$ causes a problem since it is not a gauge invariant quantity. To fix this we note the structure of the second GL equation (2.6), where the supercurrent is proportional to the dimensionless quantity $\nabla\theta(\mathbf{r}) - \frac{q}{\hbar}\mathbf{A}$. This quantity is invariant under the general gauge transformation

$$\mathbf{A} \to \mathbf{A} + \nabla\chi \quad \text{and} \quad \nabla\theta \to \nabla\theta + \frac{q}{\hbar}\nabla\chi. \tag{2.22}$$

To get the equivalent gauge transformation in the case of a phase difference instead of a phase gradient, just integrate the above expression from side 1 to side 2

$$\begin{aligned}\int_{\mathbf{r}_1}^{\mathbf{r}_2} \mathbf{A}\cdot \mathrm{d}\mathbf{r}' \to \int_{\mathbf{r}_1}^{\mathbf{r}_2} (\mathbf{A}+\nabla\chi)\cdot \mathrm{d}\mathbf{r}' &= \int_{\mathbf{r}_1}^{\mathbf{r}_2} \mathbf{A}\cdot \mathrm{d}\mathbf{r}' + \chi_2 - \chi_1,\\ \int_{\mathbf{r}_1}^{\mathbf{r}_2} \nabla\theta \to \int_{\mathbf{r}_1}^{\mathbf{r}_2} (\nabla\theta - \frac{q}{\hbar}\chi)\cdot \mathrm{d}\mathbf{r}' &= \theta_2 - \theta_1 - \frac{q}{\hbar}(\chi_2 - \chi_1),\end{aligned}$$

which tells us that the phase difference of the Josephson equations (2.20) and (2.21) in the presence of a magnetic field $\nabla \times \mathbf{A} = \mathbf{B}$ must be changed in the following manner (setting $q = 2e$)

$$\theta_2 - \theta_1 \to \gamma_{21} = \theta_2 - \theta_1 + \frac{2e}{\hbar}\int_{\mathbf{r}_2}^{\mathbf{r}_1} \mathbf{A}\cdot \mathrm{d}\mathbf{r}', \tag{2.23}$$

where we dub the quantity γ gauge invariant phase difference.

Josephson junction arrays

Connecting a large number of Josephson junctions together into a network, one gets what is called a Josephson junction array (JJA). The easiest way of picturing a JJA

is to imagine a lattice of superconducting islands connected by Josephson junctions. Such arrays show a plethora of interesting static and dynamic phenomena (see e.g. [37]), especially in a transverse magnetic field. These circumstances will, just as in type-II superconductor, cause vortices to form. But since it is energetically more favorable, the vortices will not form in the superconducting material itself, but will sit on a lattice dual to the one making up the array, that is, in the spaces between the superconducting islands. Note also that even if the superconducting grains are of type-I, vortices will still be present in such a system, since the flux penetration is happening in the material between the grains.

Now, if we think of granular superconductors, i.e., systems where grains of superconducting material are embedded in an insulating or normal metal background, it is not hard to see the resemblance with JJA:s. Also assuming that the superconducting grains are connected through Josephson junctions makes the analogy complete. JJA:s can thus serve as model systems for granular superconducting materials.

2.4 XY model

Ignoring charging effects, the energy of a two-dimensional Josephson junction array is in fact equivalent to that of a classical XY model, as will be shown later in this section. The XY model on the other hand, can be viewed as discrete version of the GL free energy functional (with certain approximations), where the coherence length ξ serves as a short-distance cutoff, since it is the shortest length possible between the grains, if one is to consider the superconducting phase at each grain as independent. This means, at least in the case of small magnetic fields where the typical vortex-vortex separation length is much larger than the coherence length ξ, that a model of a Josephson junction array will also model the properties of isotropic continuous type-II superconductors.

What now follows will be the two different ways of deriving the form of the XY model Hamiltonian discussed above. The first approach is to start from the Ginzburg-Landau free energy functional given by (2.2). Using the polar form (2.1) of the complex order parameter in that equation gives (ignoring the normal state contribution)

$$F_{GL}[\Psi(\mathbf{r})] = \int \mathrm{d}^d r \Bigg[\alpha |\Psi(\mathbf{r})|^2 + \frac{\beta}{2} |\Psi(\mathbf{r})|^4 + \frac{|\Psi(\mathbf{r})|^2}{2m} (\nabla |\Psi(\mathbf{r})|)^2 + \frac{|\Psi(\mathbf{r})|^2}{2m} (\frac{\hbar}{i} \nabla \theta(\mathbf{r}) - q\mathbf{A})^2 + \frac{\mathbf{B}^2}{2\mu_0} \Bigg].$$

To simplify this expression we assume that the amplitude of the complex order parameter is constant in space (the London approximation)

$$\Psi(\mathbf{r}) = \Psi_0 e^{i\theta(\mathbf{r})}, \tag{2.24}$$

so that the space dependence is only in the phase angle $\theta(\mathbf{r})$ (except in the vortex cores). In that approximation the third term is zero and the first two terms are just constants, so they can be ignored. Further assuming a space independent $\mathbf{B}$-field we can also throw away the last term. Now all that is left is the gradient term

$$F_{GL} \sim \int \mathrm{d}^d r \frac{\hbar^2 \Psi_0^2}{2m} (\nabla\theta(\mathbf{r}) - \frac{2e}{\hbar}\mathbf{A}(\mathbf{r}))^2. \tag{2.25}$$

Now discretize space (setting the lattice parameter to at least the coherence length ξ) and make the substitutions

$$\nabla\theta(\mathbf{r}) \to \theta_i - \theta_j \quad \text{and} \quad \int \mathrm{d}^d r \to \sum_{\langle ij \rangle}, \tag{2.26}$$

which are correct up to some dimensionally dependent constants ($\langle ... \rangle$ denotes a sum over all links between lattice points in the system). This gives us the Hamiltonian

$$H = \sum_{\langle ij \rangle} J_{ij} \gamma_{ij}^2, \tag{2.27}$$

where the coupling $J_{ij} = \hbar^2 \Psi_0^2 / m$ is just a constant in this derivation, but can in general be different from link to link. We have also made the substitution to the gauge invariant phase difference γ_{ij} given by (2.23). The problem with this expression is that it does not reflect the original periodicity of the phase angles, i.e. it is not invariant under a local 2π rotation of a phase angle. To fix this one can instead choose the final form of the XY model Hamiltonian to be

$$H = -\sum_{\langle ij \rangle} J_{ij} \cos\gamma_{ij}, \tag{2.28}$$

where the cosine function is chosen since it is both 2π-periodic and has the proper Taylor expansion ($\cos x = 1 - x^2 + O(x^4)$). In that sense this form represents the simplest possible model of a type-II superconductor, in which vortices also can exist.

Start now instead from the two Josephson relations (2.20) and (2.21) in their gauge invariant form. The energy e_{ij} stored in one junction can be calculated by simply integrating the electrical power $I_{ij}^s V_{ij}$ over time

$$e_{ij} = \int \mathrm{d}t I_{ij}^s V_{ij} = \frac{\hbar I_{ij}^c}{2e} \int \mathrm{d}t \dot{\gamma}_{ij} \sin\gamma_{ij} \sim \frac{\hbar I_{ij}^c}{2e} \cos\gamma_{ij} \equiv J_{ij} \cos\gamma_{ij}, \tag{2.29}$$

giving a result equivalent to (2.28). The coupling constant $J_{ij} = \hbar I_{ij}^c / 2e$ is in this context also called the Josephson energy E_{ij}^J of the junction. Comparing this relation with the one obtained from (2.27), gives the critical current of a junction as $I_{ij}^c = 2e\hbar\Psi_0^2/m$ (this has the correct dimensions of a current i two dimensions).

2.5 Non-equilibrium phenomena

The study of transport phenomena requires methods outside the normal equilibrium thermodynamics toolbox. In this section some these concepts in non-equilibrium thermodynamics will be introduced. The reciprocal relations due to Onsager will be discussed and applied specifically to the case of thermoelectric transport. A derivation due to Kubo [38] of the very useful formulas bearing his name will also be given. Although the derivation is made for classical Hamiltonian dynamics, the end result is still valid for the type of stochastic dynamics we employ in our simulations.

Onsager relations

Begin with a system described macroscopically by some extensive state variables x_i and with an entropy $S = S(x_1, x_2, ...)$, which depends on all of these. In equilibrium S is maximized, i.e.,

$$\frac{\partial S}{\partial x_i} = 0, \quad \text{for} \quad x_i = \bar{x}_i, \tag{2.30}$$

where $\bar{x}_i$ is the equilibrium value of the state variable x_i. Consider now small fluctuations away from equilibrium and Taylor expand S to lowest order

$$S = S_0 - \frac{1}{2}\sum_{ij}(x_i - \bar{x}_i)c_{ij}(x_j - \bar{x}_j), \quad c_{ij} = \left.\frac{\partial^2 S}{\partial x_i x_j}\right|_{x_i=\bar{x}_i, x_j=\bar{x}_j}. \tag{2.31}$$

Define generalized thermodynamic forces X_i conjugate to x_i by

$$X_i = \frac{\partial S}{\partial x_i} = -c_{ij}(x_j - \bar{x}_j), \tag{2.32}$$

where we have used the expansion above in the second equality. Intuitively we expect that the time dependence of the x_i:s should depend on the X_k:s, $\dot{x}_i = f(X_1, X_2, ...)$. For small fluctuations we assume that this relation is linear

$$\dot{x}_i = \sum_j L_{ij} X_j, \tag{2.33}$$

where L_{ij} are called kinetic coefficients. In 1931 Onsager showed in two seminal papers [39, 40] that, as a consequence of microscopic reversibility of the equations of motions for the state variables x_i, the kinetic coefficients obey the symmetry relation

$$L_{ij}(\mathbf{B}) = \epsilon_i \epsilon_j L_{ji}(-\mathbf{B}), \tag{2.34}$$

in a magnetic field $\mathbf{B}$, and where $\epsilon_i = \pm 1$ depending on whether the variable x_i is even or odd under time reversal. This relation is known as Onsager's symmetry or reciprocal relation or just Onsager's relation.

For the Onsager relations to be of any use, we must for a particular system first find the generalized forces X_i conjugate to the state variables x_i. To do this, first note that the time derivative of the entropy is

$$\dot{S} = \sum_i \frac{\partial S}{\partial x_i}\dot{x}_i = \sum_i X_i \dot{x}_i. \tag{2.35}$$

The total entropy S is just the entropy density $s(\mathbf{r})$ integrated over the system

$$S = \int s(\mathbf{r})dV, \quad s(\mathbf{r}) = \sum_i X_i(\mathbf{r})\rho_i(\mathbf{r}), \tag{2.36}$$

where $\rho_i(\mathbf{r})$ is the density of x_i. From the last two equations it is clear that once you have written down an expression for $\dot{s}$, you have also found the proper thermodynamic forces of the system and can make use of the symmetry relations given by Onsager.

Thermoelectric transport

Let us now try to do this for a specific case, namely that of a system where we consider thermoelectric transport alone. Assuming that we are locally close to equilibrium, the first law of thermodynamics reads

$$de = Tds + \xi dn, \tag{2.37}$$

where e is the energy density, s the entropy density, n the particle density, T is the temperature and ξ the full electrochemical potential ($\xi = \mu + q\phi$, where μ is the chemical potential, ϕ the electrostatic potential, and q the charge of a particle associated with the density n). Further we assume that the energy density e obeys a continuity equation $\dot{e} + \nabla \cdot \mathbf{J}_E = 0$, and the same for n. In general we have local entropy production, so that $\dot{s} + \nabla \cdot \mathbf{J}_S = \sigma_S$, but this source term does not affect the currents and will therefore be omitted in what follows.

Look now at the time derivative of e given by (2.37),

$$\dot{e} = T\dot{s} + \xi\dot{n}, \tag{2.38}$$

which after insertion of the continuity equations for the densities becomes

$$\mathbf{J}^E = T\mathbf{J}^S + \xi\mathbf{J}^N = \mathbf{J}^Q + \xi\mathbf{J}^N, \tag{2.39}$$

having defined the heat current density as $\mathbf{J}_Q = T\mathbf{J}_S$. From this expression we have

$$\dot{s} = -\nabla \cdot \mathbf{J}^S = -\nabla \cdot \left(\frac{1}{T}\mathbf{J}^E\right) + \nabla \cdot \left(\frac{\xi}{T}\mathbf{J}^N\right). \tag{2.40}$$

Using the fact that $\nabla \cdot \mathbf{J}^E = \nabla \cdot \mathbf{J}^N = 0$ (since $\dot{e} = \dot{n} = 0$) in a stationary state yields

$$\dot{s} = -\nabla\left(\frac{1}{T}\right) \cdot \mathbf{J}^E + \nabla\left(\frac{\mu}{T}\right) \cdot \mathbf{J}^N, \tag{2.41}$$

which can also be expressed as

$$\dot{s} = -\nabla\left(\frac{1}{T}\right) \cdot \mathbf{J}^Q + \left(\frac{-1}{T}\right)\nabla\xi \cdot \mathbf{J}^N, \tag{2.42}$$

by the use of (2.39). These two equations can be compared with (2.35). Focusing on the last equation and making the identifications

$$\dot{x}_1, \dot{x}_2 \to \mathbf{J}^N, \mathbf{J}^Q \quad \text{and} \quad X_1, X_2 \to \left(\frac{-1}{T}\right)\nabla\xi, \nabla\left(\frac{1}{T}\right), \tag{2.43}$$

gives from the definition of the kinetic coefficients (2.33) the following linear relations between the particle and heat current density responses to electrochemical potentials and thermal gradients

$$\mathbf{J}^N = L_{NN}\left(\frac{-1}{T}\right)\nabla\xi + L_{NQ}\nabla\left(\frac{1}{T}\right), \tag{2.44}$$

$$\mathbf{J}^Q = L_{QN}\left(\frac{-1}{T}\right)\nabla\xi + L_{QQ}\nabla\left(\frac{1}{T}\right), \tag{2.45}$$

with an Onsager relation

$$L_{NQ} = L_{QN}, \tag{2.46}$$

from (2.34), since both $\mathbf{J}_N$ and $\mathbf{J}_Q$ are currents and therefore odd with repect to time reversal. More specific thermoelectric transport coefficients can now be expressed in terms of the kinetic coefficients using these equations. By the use of the Onsager relation (2.46) connections between some of the coefficients can also be made.

Linear response and the Kubo formula

Consider a classical system in equilibrium with a Hamiltonian H_0. Now add a small perturbation H' to it, so that the total Hamiltonian H is

$$H = H_0 + H' = H - f_A(t)A, \tag{2.47}$$

where A is a classical dynamical variable and $f_A(t)$ a time-dependent external field. This represents a general mechanical perturbation, where we can think of $f_A(t)$ as a generalized force and A as the quantity which couples to this force. A typical

question one might ask is how this perturbation will affect some other observable $B(t)$ in the system. To answer this, let us first consider the more general question of how the equilibrium probability density ρ_{eq}, given by the unperturbed Hamiltonian H_0, will change.

In classical mechanics the time evolution of a probability density $\rho(\mathbf{p}, \mathbf{q})$ ($(\mathbf{p}, \mathbf{q})$ is a short-hand notation for all the canonical variables of the system) is given by the Liouville equation

$$\partial_t \rho = \{H, \rho\} \equiv -\mathcal{L}\rho, \tag{2.48}$$

with $\mathcal{L}$ being the so called Liouville operator and $\{H, \rho\}$ is a Poisson bracket defined by

$$\{H, \rho\} = \sum_i \left(\frac{\partial H}{\partial q_i} \frac{\partial \rho}{\partial p_i} - \frac{\partial \rho}{\partial q_i} \frac{\partial H}{\partial p_i} \right). \tag{2.49}$$

Since $\mathcal{L}$ is a linear operator we get for the perturbed system

$$\partial_t \rho = \{H_0 + H', \rho\} = \{H_0, \rho\} + \{H', \rho\} = -\mathcal{L}_0 \rho - \mathcal{L}' \rho. \tag{2.50}$$

In what follows, we assume that the system is in equilibrium until the perturbation is turned on at time $t = t_0$, i.e., $f_A(t) = 0$ for $t < t_0$ and $\rho(t_0) = \rho_{eq}$. Continue by expanding ρ to first order (this is the *linear* in linear response) in the perturbation parameter f_A

$$\rho(t) = \rho_{eq} + \rho' + O(f_A^2). \tag{2.51}$$

Taking the time derivative of the above equation gives

$$\partial_t \rho = \partial_t \rho_{eq} + \partial_t \rho' = -(\mathcal{L}_0 + \mathcal{L}')(\rho_{eq} + \rho') + ... \tag{2.52}$$

Note that $\mathcal{L}'\rho'$ is second order in f_A and therefore can be neglected and that $-\mathcal{L}_0 \rho_{eq} = \partial_t \rho_{eq}$, so that this term can be subtracted from both sides. With these simplifications we get

$$\partial_t \rho' = -\mathcal{L}_0 \rho' - \mathcal{L}' \rho_{eq}. \tag{2.53}$$

This is a nonhomogeneous first-order differential equation, which can be solved easily to get ρ' by transforming to Fourier space and then applying the convolution theorem in the backward transform. The solution is

$$\rho'(t) = -\int_{t_0}^{t} dt' e^{-(t-t')\mathcal{L}_0} \mathcal{L}'(t') \rho_{eq}. \tag{2.54}$$

But since we know that $\rho_{eq} = e^{-\beta H_0}/Z$ and $H' = -f_A A$, the factor $\mathcal{L}'(t')\rho_{eq}$ can be explicitly calculated

$$\begin{aligned} -\mathcal{L}'(t')\rho_{eq} = \{H', \rho_{eq}\} = f_A(t') \frac{1}{Z} \{A, e^{-\beta H_0}\} = \\ f_A(t') \frac{1}{Z} \sum_i \left(\frac{\partial A}{\partial q_i} \frac{\partial e^{-\beta H_0}}{\partial p_i} - \frac{\partial e^{-\beta H_0}}{\partial q_i} \frac{\partial A}{\partial p_i} \right) = \\ \beta f_A(t') \frac{e^{-\beta H_0}}{Z} \{A, H_0\} = \beta f_A(t') \rho_{eq} \dot{A}. \end{aligned}$$

Consider now the initial question of the response of some observable B to the perturbation at time $t = t_0$

$$\delta\langle B(t)\rangle = \langle B(t)\rangle - \langle B(t_0)\rangle = \int d\mathbf{p}d\mathbf{q}B(\mathbf{p},\mathbf{q})(\rho(t) - \rho(t_0)). \tag{2.55}$$

From the calculations above we know what $\rho'(t) = \rho(t) - \rho(t_0)$ is. Inserting this in the above equation gives

$$\begin{aligned}
\delta\langle B(t)\rangle &= -\int_{t_0}^{t} dt' \int d\mathbf{p}d\mathbf{q}B(\mathbf{p},\mathbf{q})e^{-(t-t')\mathcal{L}_0}\mathcal{L}'(t')\rho_{eq} \\
&= \int_{t_0}^{t} dt' \int d\mathbf{p}d\mathbf{q}B(\mathbf{p},\mathbf{q})e^{-(t-t')\mathcal{L}_0}\beta f_A(t')\rho_{eq}\dot{A}(t_0) \\
&= \beta\int_{t_0}^{t}\langle B(t-t')\dot{A}(t_0)\rangle f_A(t')dt'.
\end{aligned}$$

To get to the final expression, we have used the fact that the phase space integral over ρ_{eq} becomes an equilibrium average and that the exponential Liouville operator $e^{-(t-t')\mathcal{L}_0}$ can work backwards on $B(\mathbf{p},\mathbf{q})$ making it time dependent $B(\mathbf{p},\mathbf{q};t-t')$ if $B(\mathbf{p},\mathbf{q})$ has no explicit time dependence. This is true since the solution of $\partial_t\rho = \mathcal{L}_0\rho$ is $\rho(t) = e^{-t\mathcal{L}_0}\rho(0)$. If we make the substitution $s = t - t'$ and , we get to the standard form of a Kubo formula.

$$\delta\langle B(t)\rangle = \int_0^t \phi_{BA}(s)f_A(t-s)ds, \quad \phi_{BA}(s) = \beta\langle B(s)\dot{A}(0)\rangle. \tag{2.56}$$

The result is quite astonishing - the dynamics of the linear response is given by an equilibrium correlation function. This is related to something called Onsager's regression law, which states that for small deviations from equilibrium, the relaxation towards equilibrium is governed by equilibrium fluctuations. The physical reason for this can be understood from the following argument. Since fluctuations from equilibrium can be the result of either a small perturbation or spontaneous fluctuations, the dynamics of the relaxation towards equilibrium should follow the same laws in both cases.

Kubo formula for electric conductivity

Note how (2.56) is just the convolution of ϕ_{BA} and f_A, so that the frequency dependent response is given by

$$\delta\langle B(\omega)\rangle = \phi_{BA}(\omega)f_A(\omega), \tag{2.57}$$

where $\phi_{BA}(\omega)$ and $f_A(\omega)$ are the Fourier transforms of the corresponding quantities. As an example we can try to calculate the frequency dependent electric conductivity given by Ohm's law $J_{ij}(\omega) = \sigma_{ij}(\omega)E_j(\omega)$. Here we can identify B

from the derivation above as the current density $\mathbf{J}$ and the perturbing force $f_A(t)$ as the electric field $\mathbf{E}$. $\mathbf{E}$ couples to the polarization density $\mathbf{P}$ to give the total perturbing Hamiltonian

$$H' = -\int \mathbf{E}(t) \cdot \mathbf{P} d\Omega = -\Omega \mathbf{P} \cdot \mathbf{E}(t), \tag{2.58}$$

where Ω is the volume of the system and we have assumed that $\mathbf{P}$ has no spatial dependence. We can identify $\Omega\mathbf{P}$ as A in previous calculations. Furthermore $\dot{\mathbf{P}} = \mathbf{J}$, leading to the following Kubo formula for the electrical conductivity

$$\sigma_{ij}(\omega) = \frac{\Omega}{k_B T} \int_0^\infty \langle J_i(t) J_j(0) \rangle e^{i\omega t} dt. \tag{2.59}$$

We can also take the $\omega \to 0$ limit to get the DC conductivity as

$$\sigma_{ij} = \sigma_{ij}(\omega \to 0) = \frac{\Omega}{k_B T} \int_0^\infty \langle J_i(t) J_j(0) \rangle dt. \tag{2.60}$$

Other Kubo formulas

Kubo formulas for other repsonse coefficients can be derived in a similar fashion from (2.56) for all mechanical perturbations on the form given by (2.47). In cases where the perturbation is not mechanical, for example if we want to calculate the heat conductivity by measuring the response of the heat current to a small temperature gradient, the derivation given above is not valid. Luttinger [41] showed that a thermal perturbation can be recast in a mechanical form and the heat conductivity κ therefore is given by the expected integral over a heat current density – heat current density correlation function

$$\kappa_{ij} = \frac{\Omega}{k_B T^2} \int_0^\infty \langle J_i^Q(t) J_j^Q(0) \rangle dt. \tag{2.61}$$

Analogously, the Nernst signal e_N, being the response of an electric field E_y to a thermal gradient $\nabla_x T$ in a transverse magnetic field, is given by the Kubo formula

$$e_N = \frac{\Omega}{k_B T^2} \int_0^\infty \langle E_y(t) J_x^Q(0) \rangle dt. \tag{2.62}$$

Another approach, different from Luttinger's, is to reformulate the problem using functional integrals and study the effect of a thermal perturbation. In Paper II we in this way are able to rederive the form of the above Kubo formula for e_N and as an added bonus find an expression for the heat current.

Chapter 3

Models and methods

In this chapter an in-depth discussion about the main theoretical models used in Paper I and II will be given.

Our aim here is to formulate a model for two-dimensional granular superconducting systems, valid for any type of lattice, perfectly ordered square lattices as well as structures with geometric disorder, which might be closer to real life systems. Our model is based on a phase only description, assuming a constant amplitude of the superconducting order parameter and consequently that the important fluctuations are those of the phase. The model is explicitly constructed to measure the Nernst effect, and that requires some special boundary conditions. These are discussed in the first part of this chapter. The second part is a review of the type of dynamics we have employed and the implementation of these.

3.1 Magnetic vector potential and electric field

The construction of the gauge potential is an integral part of our model. We choose to separate the magnetic vector potential into two parts

$$\mathbf{A}(\mathbf{r},t) = \mathbf{A}_{\text{ext}}(\mathbf{r}) + \frac{\Phi_0}{2\pi}\mathbf{\Delta}(t), \tag{3.1}$$

where $\mathbf{A}_{\text{ext}}(\mathbf{r})$ is only space dependent, while $\mathbf{\Delta}(t)$ is only time dependent. In this way $\mathbf{A}_{\text{ext}}$ corresponds to a constant and spatially uniform magnetic field

$$\mathbf{B} = \nabla \times \mathbf{A} = \nabla \times \mathbf{A}_{\text{ext}}, \tag{3.2}$$

which is transverse to our two-dimensional system if make the gauge choice $\mathbf{A}_{\text{ext}}(\mathbf{r}) = B_z x\hat{\mathbf{y}}$, so that $\mathbf{B} = B_z\hat{\mathbf{z}}$. The second part $\mathbf{\Delta} = (\Delta_x, \Delta_y)$, on the other hand, describes temporal fluctuations in a spatially uniform electric field

$$\mathbf{E} = -\dot{\mathbf{A}} = -\frac{\Phi_0}{2\pi}\dot{\mathbf{\Delta}}. \tag{3.3}$$

This $\mathbf{E}$ should be interpreted not as the local electric field in the model, but rather as the average field across the system obtained from the total voltage across the system divided by the linear system size L. The voltage between two lattice points i and j is defined by the second Josephson equation (2.21) in its gauge invariant form (here setting $q = -2e$ and denoting $(2\pi/\Phi_0)\int_i^j \mathbf{A}\cdot d\mathbf{r}' = A_{ij}$)

$$V_{ij} = \frac{\hbar}{2e}\dot{\gamma}_{ij} = \frac{\hbar}{2e}(\dot{\theta}_i - \dot{\theta}_j - \dot{A}_{ij}) = \frac{\hbar}{2e}(\dot{\theta}_i - \dot{\theta}_j - \dot{\mathbf{\Delta}}\cdot\mathbf{r}_{ji}), \tag{3.4}$$

where $\mathbf{r}_{ji} = \mathbf{r}_j - \mathbf{r}_i$ is the vector from i to j. So to get the total voltage across the system say in the y-direction we must set $\mathbf{r}_j = \mathbf{r}_i + L\hat{\mathbf{y}}$. If we use periodic boundary conditions, the time derivative of the phases will cancel and we get

$$V_y = -\frac{\hbar}{2e}L\dot{\Delta}_y, \tag{3.5}$$

which is zero if $\mathbf{\Delta}$ is set to zero. We must thus include $\mathbf{\Delta}$ in the vector potential, if we at the same time as using periodic boundary conditions want to measure the electric field across the system. The dynamic $\mathbf{\Delta}$-field is also called fluctuating twist boundary conditions (FTBC) [42], since it is essentially just the phase twist per unit length in the system.

In our simulations the integrated magnetic vector potential A_{ij} is calculated by integrating $\mathbf{A}$ along the vector $\mathbf{r}_{ji}$ from i to j. This is done by simply parametrizing the integration path in a standard way:

$$\mathbf{r}'(t) = \mathbf{r}_i + (\mathbf{r}_j - \mathbf{r}_i)t \quad t: 0 \to 1. \tag{3.6}$$

The integral can then be easily calculated

$$A_{ij} = \frac{2\pi}{\Phi_0}\int_{\mathbf{r}_i}^{\mathbf{r}_j}\mathbf{A}\cdot\mathrm{d}\mathbf{r}' = \frac{2\pi}{\Phi_0}\int_{t=0}^{1}\mathbf{A}'\frac{d\mathbf{r}'}{dt}\mathrm{d}t + \mathbf{\Delta}\cdot(\mathbf{r}_j - \mathbf{r}_i), \tag{3.7}$$

where the first term is equal to

$$B_z(y_j - y_i)\frac{1}{2}(x_i + x_j).$$

The final expression for the integrated magnetic vector potential with our gauge choice thus becomes

$$A_{ij} = \frac{2\pi}{\Phi_0}B_z y_{ji}x^c_{ij} + \mathbf{\Delta}\cdot\mathbf{r}_{ji}, \tag{3.8}$$

with the definitions $y_{ji} = y_j - y_i$, $x^c_{ij} = (x_i + x_j)/2$, and $\mathbf{r}_{ji} = \mathbf{r}_j - \mathbf{r}_i$ as before.

3.2 Periodic boundary conditions in our gauge

To avoid severe finite size effects it is favorable to use periodic boundary conditions in all directions. This however induces another problem, since the spatially dependent part of the magnetic vector potential in our gauge is $\mathbf{A}(\mathbf{r}) = \mathbf{A}_{\text{ext}} = B_z x\hat{\mathbf{y}}$

and thus non-periodic

$$\mathbf{A}(\mathbf{r} + L_x\hat{\mathbf{e}}_x) - \mathbf{A}(\mathbf{r}) = B_z L_x \hat{\mathbf{y}}. \tag{3.9}$$

Using PBC we must require that all physical quantities share this periodicity, i.e., are single valued. Consider the continuum case, where the gauge invariant quantity $\nabla\theta(\mathbf{r}) + \frac{2e}{\hbar}\mathbf{A}(\mathbf{r})$ (with $q = -2e$) is related to the supercurrent through the second GL equation (2.6). This quantity must therefore be periodic

$$\nabla\theta(\mathbf{r} + \mathbf{L}) + \mathbf{A}(\mathbf{r} + \mathbf{L}) = \nabla\theta(\mathbf{r}) + \mathbf{A}(\mathbf{r}), \qquad \mathbf{L} = L_i\hat{\mathbf{i}} \quad i = x, y. \tag{3.10}$$

We have here dropped all constants, which are anyway unimportant to this argument. This is possible if we make the phases non-periodic

$$\theta(\mathbf{r} + \mathbf{L}) - \theta(\mathbf{r}) = F_i. \tag{3.11}$$

To find the compensating terms F_i, take the gradient of equation (3.11) to get

$$\begin{aligned}
\nabla F_x &= \nabla\theta(\mathbf{r} + L_x\hat{\mathbf{x}}) - \nabla\theta(\mathbf{r}) = \mathbf{A}(\mathbf{r}) - \mathbf{A}(\mathbf{r} + L_x\hat{\mathbf{x}}) = -B_z L_x\hat{\mathbf{y}} \\
\nabla F_y &= \nabla\theta(\mathbf{r} + L_y\hat{\mathbf{y}}) - \nabla\theta(\mathbf{r}) = \mathbf{A}(\mathbf{r}) - \mathbf{A}(\mathbf{r} + L_y\hat{\mathbf{y}}) = 0,
\end{aligned}$$

where we have inserted Eq. (3.10) to get the last equality. Simply integrating these equations yields the compensating terms

$$F_x = -B_z L_x y \qquad \text{and} \qquad F_y = 0, \tag{3.12}$$

where the integration constants have been set to zero. So, when taking the phase difference $\theta_i - \theta_j$, where the vector $\mathbf{r}_{ji}$ from i to j goes across the system boundary in the *positive* x-direction, a term $-F_x$ should be added to this difference. If $\mathbf{r}_{ji}$ goes in the *negative* x-direction the term $+F_x$ should be added.

3.3 Langevin dynamics

The simplest approach to constructing dynamical equations for the phases $\{\theta_i\}$ and the twist variables $\mathbf{\Delta} = (\Delta_x, \Delta_y)$, are the so called Langevin dynamics, in the literature also often referred to as time dependent Ginzburg-Landau (TDGL) [43, 44] or model A [45] dynamics. We start from the Hamiltonian of the XY model (2.28), which can be used to model Josephson junction networks or even bulk type-II superconductors under certain assumptions, as discussed previously. It is natural to assume that, for small deviations from equilibrium, the time derivative of the a phase variable $\dot{\theta}_i$ is proportional to the derivative of the XY model Hamiltonian $\partial H_{XY}/\partial\theta_i$. Nevertheless, there is also the effect of thermodynamical fluctuations to consider. This is done by adding a thermal noise term, so that the equations of motion for the phases $\{\theta_i\}$ takes on the Langevin form

$$\hbar\dot{\theta}_i = -\Gamma^\theta \frac{\partial H}{\partial\theta_i} + \eta_i^\theta. \tag{3.13}$$

where Γ^θ is a dimensionless constant setting the rate of relaxation towards the local energy minimum. The thermal noise terms η_i^θ must be chosen in such way that it gives the correct equilibrium Boltzmann distribution for the equal time correlators. This is assured if the noise term is Gaussian white-noise correlated satisfying

$$\langle \eta_i^\theta(t) \rangle = 0 \quad \text{and} \quad \langle \eta_i^\theta(t) \eta_j^\theta(t') \rangle = 2\hbar\Gamma^\theta k_B T \delta_{ij} \delta(t-t'). \tag{3.14}$$

The equations of motion for the twist variables $\boldsymbol{\Delta} = (\Delta_x, \Delta_y)$ are on the very same form

$$\hbar \dot{\boldsymbol{\Delta}} = -\Gamma^\Delta \frac{\partial H}{\partial \boldsymbol{\Delta}} + \boldsymbol{\eta}^\Delta. \tag{3.15}$$

Here the constant Γ^Δ is no longer dimensionless, but has the dimension of length^{-2}, since $[\boldsymbol{\Delta}] = \text{length}^{-1}$, being the phase twist per unit length in the system. For simplicity we set $\Gamma^\Delta = \Gamma^\theta / L^2$. The thermal noise term $\boldsymbol{\eta}^{\Delta_i}$ has the correlations

$$\langle \eta^\Delta(t) \rangle = 0 \quad \text{and} \quad \langle \eta_\mu^\Delta(t) \eta_\nu^\Delta(t') \rangle = 2\hbar\Gamma^\Delta k_B T \delta_{\mu\nu} \delta(t-t'). \tag{3.16}$$

While the equations of motions (3.13) and (3.15) for $\{\theta_i\}$ and $\boldsymbol{\Delta}$ are on a simple enough form, they can be rewritten to remind us of that they in fact describe a network of Josephson junctions. In this alternative view the equations of motion look like

$$\gamma \dot{\theta}_i = -\frac{1}{2e} \sum_{j \in \mathcal{N}_i} I_{ij}^s + \eta_i, \tag{3.17}$$

$$\gamma_\Delta \dot{\boldsymbol{\Delta}} = \frac{1}{2e} \sum_{\langle ij \rangle} I_{ij}^s \mathbf{r}_{ji} + \boldsymbol{\zeta}, \tag{3.18}$$

where $I_{ij}^s = I_{ij}^c \sin(\theta_i - \theta_j - A_{ij})$ is the Josephson supercurrent from grain i to j with a critical current $I_{ij}^c = 2eJ_{ij}/\hbar$. The sum in the first equation runs over the set $\mathcal{N}_i$ of superconducting grains connected to i, while it runs over all links in the system in the second one and $\mathbf{r}_{ji} = \mathbf{r}_j - \mathbf{r}_i$. The time constant γ is dimensionless and $\gamma_\Delta = \gamma L^2$. The Gaussian white noise terms η_i and $\boldsymbol{\zeta}$ now have the correlations

$$\langle \eta_i \rangle = 0, \quad \langle \eta_i(t) \eta_j(t') \rangle = (2k_B T\gamma/\hbar)\delta_{ij}\delta(t-t') \tag{3.19}$$

$$\langle \boldsymbol{\zeta}(t) \rangle = 0, \quad \langle \zeta_\mu(t) \zeta_\nu(t') \rangle = (2k_B T\gamma_\Delta/\hbar)\delta_{\mu\nu}\delta(t-t'). \tag{3.20}$$

3.4 RSJ dynamics

In RSJ dynamics one models a Josephson junction network or granular superconductor as an electrical circuit, where every junction is shunted by a resistance R (see Fig. 3.1). We write the total current from site i to site j as a sum of the following contributions

$$I_{ij}^{\text{tot}} = I_{ij}^c \sin\gamma_{ij} + \frac{V_{ij}}{R} + I_{ij}^n \equiv I_{ij}^s + I_{ij}^r + I_{ij}^n. \tag{3.21}$$

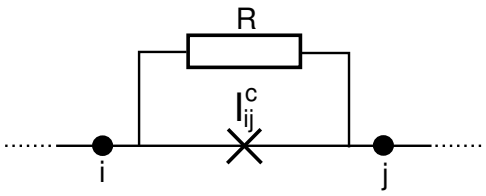

Figure 3.1: Circuit equivalent to RSJ dynamics.

The first term is simply the supercurrent through junction given by (2.20) and the second one the current through the resistor R, with the Josephson voltage from (2.21)

$$V_{ij} = \frac{\hbar}{2e}\dot{\gamma}_{ij} = \frac{\hbar}{2e}(\dot{\theta}_i - \dot{\theta}_j - \dot{A}_{ij}). \tag{3.22}$$

Further I^n_{ij} is the Johnson-Nyquist noise [46, 47] in the resistor with the properties

$$\langle I^n_{ij}(t)\rangle = 0 \quad \text{and} \quad \langle I^n_{ij}(t)I^n_{kl}(t')\rangle = \frac{2k_BT}{R}(\delta_{ik}\delta_{jl} - \delta_{il}\delta_{jk})\delta(t-t'). \tag{3.23}$$

We proceed by demanding local conservation of the total current

$$\sum_{i\in\mathcal{N}_j} I^{\text{tot}}_{ij} = 0, \tag{3.24}$$

where the sum is taken over the set $\mathcal{N}_i$ of all nearest neighbors to site i. This gives the equations of motion for the phases

$$\sum_{j\in\mathcal{N}_i} \frac{\hbar}{2eR}(\dot{\theta}_i - \dot{\theta}_j - \dot{A}_{ij}) = -\sum_{j\in\mathcal{N}_i}(I^c_{ij}\sin(\theta_i - \theta_j - A_{ij}) + I^n_{ij}). \tag{3.25}$$

The dynamical equation for $\mathbf{\Delta}$ is generated by fixing the average current density $\bar{\mathbf{J}}^{\text{ext}}$ in the system. We define this average current density as

$$\bar{\mathbf{J}}^{\text{ext}} = \frac{1}{L^2}\int \mathbf{J}(\mathbf{r})d^2r, \tag{3.26}$$

where $\mathbf{J}(\mathbf{r})$ is the current density in the system, which in a circuit model must be defined only on the links connecting the lattice points

$$\mathbf{J}(\mathbf{r}) = \sum_{\langle ij\rangle}\int_{\mathbf{r_i}}^{\mathbf{r_j}} I^{\text{tot}}_{ij}\delta(\mathbf{r}-\mathbf{r}')d\mathbf{r}'. \tag{3.27}$$

Inserting this definition, the average current density becomes

$$\bar{\mathbf{J}}^{\text{ext}} = \frac{1}{L^2}\int \mathbf{J}(\mathbf{r})d^2r = \frac{1}{L^2}\sum_{\langle ij\rangle} I^{\text{tot}}_{ij}\mathbf{r}_{ji}, \tag{3.28}$$

where $\mathbf{r}_{ji} = \mathbf{r}_j - \mathbf{r}_i$ as before. Using the definition of the total current (3.21), the equation of motion for $\mathbf{\Delta}$ can be expressed as

$$\sum_{\langle ij \rangle} \frac{\hbar}{2eR}(\dot{\theta}_i - \dot{\theta}_j - \dot{\mathbf{\Delta}} \cdot \mathbf{r}_{ji})\mathbf{r}_{ji} = L^2 \bar{\mathbf{J}}^{\text{ext}} - \sum_{\langle ij \rangle}(I_{ij}^c \sin(\theta_i - \theta_j - \dot{\mathbf{\Delta}} \cdot \mathbf{r}_{ji}) + I_{ij}^n)\mathbf{r}_{ji}. \quad (3.29)$$

3.5 Circuit model of Langevin dynamics

In the light of the description of RSJ dynamics we can go ahead and interpret the Langevin dynamical equations (3.17) and (3.18) as the equations of motion for a Josephson junction network where each grain is connected to a resistance R_0 to ground (see Fig. 3.2). The equation of motion for the phases (3.17) is generated

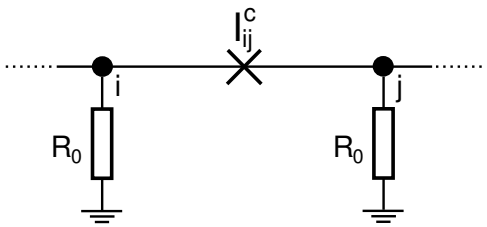

Figure 3.2: The circuit equivalent to Langevin dynamics.

by proceeding in the same fashion as for RSJ dynamics and demanding current conservation at each grain i

$$\sum_{j \in \mathcal{N}_i} I_{ij}^s + \frac{\hbar}{2eR_0}\dot{\theta}_i + I_i^n = 0, \quad (3.30)$$

where $V_i = \hbar\dot{\theta}_i/2e$ is the voltage to ground over the resistor R_0 and I_i^n is the Johnson-Nyquist noise current in this resistor properties $\langle I_i^n(t) \rangle = 0$ and $\langle I_i^n(t) I_j^n(t') \rangle = (2k_B T/R_0)\delta_{ij}\delta(t - t')$. By regrouping the above equation and identifying the dimensionless time constant as $\gamma = \hbar/(R_0(2e)^2)$ we obtain exactly the equation of motion for the phases as given previously by (3.17).

The equations of motion for $\mathbf{\Delta}$ can be realized by adding a resistance $R_\parallel$ parallel to the whole array in both directions, acting as a normal current channel, and fixing the average total current through the system given by $L\bar{\mathbf{J}}^{\text{ext}}$. This total current is the sum of the supercurrents in the system plus the normal current and the noise current through the parallel resistor, giving the relation

$$L\bar{\mathbf{J}}^{\text{ext}} = \frac{1}{L}\sum_{\langle ij \rangle} I_{ij}^s \mathbf{r}_{ji} - \frac{\hbar}{2eR_\parallel} L\dot{\mathbf{\Delta}} + I^n. \quad (3.31)$$

Now, setting $\bar{\mathbf{J}}^{\text{ext}} = 0$ and $R_\parallel = R_0$ and regrouping reproduces (3.18) exactly, with the previous definition of the time constant $\gamma_\Delta = \gamma L^2 = L^2\hbar/(R_0(2e)^2)$.

Connection between Langevin and RSJ dynamics

It is possible to understand the connection between Langevin and RSJ dynamics by considering their corresponding circuit models discussed above. In the Langevin case, the resistance R_0 to ground at each site can be physically interpreted as a normal current leakage from each grain to the substrate. The RSJ model does not allow for such a leakage but instead considers the normal current through each junction by adding a parallel resistance R to the junction. The Langevin and RSJ dynamics can thus be viewed as two different limits of the same circuit model - one with both on-site resistances R_0 to ground and shunt resistances R parallel to each junction as well as a resistance $R_\parallel = R_0$ parallel to the entire array. In the limit where we take the shunt resistances R to be much larger than the resistances to the ground, i.e., $R >> R_0 = R_\parallel$, so that the normal current only goes through $R_\parallel$ and through R_0 to ground, we get the Langevin dynamics expressed in (3.17) and (3.18). The opposite limit $R << R_0 = R_\parallel$ gives a Josephson junction array well described by the RSJ dynamical equations (3.25) and (3.29). In reality the limit $R << R_0$ is usually closest to the truth, which should make RSJ dynamics the more realistic model [48].

3.6 Simulations

Forward Euler scheme

Consider a general overdamped Langevin equation on the form

$$\dot{x}(t) = f(x(t)) + \eta(t), \tag{3.32}$$

where the stochastic force term $\eta(t)$ has zero mean and correlation $\langle \eta(t)\eta(t')\rangle \sim \delta(t-t')$. The simplest possible way to simulate this equation on a computer is to discretize time in units of Δt and approximate the time derivative as a forward difference

$$\dot{x}(t) \approx \frac{1}{\Delta t}(x(t+\Delta t) - x(t)), \tag{3.33}$$

giving the so called forward Euler integration scheme

$$x(t+\Delta t) \approx x(t) + \Delta t f(x(t)) + \Delta t \eta(t). \tag{3.34}$$

In the purely deterministic case, with $\eta = 0$, this scheme has an error in each update step of the order of $(\Delta t)^2$. However, with a nonzero η we have to consider the fact that the stochastic noise is delta function correlated. Since we want to preserve the defining property of the delta function also in the discrete time case

$$\int f(t)\delta(t-t')dt = f(t') \quad \rightarrow \quad \sum f_t \hat{\delta}(t-t')\Delta t = f_{t'}, \tag{3.35}$$

we must define the discrete version of the delta function as $\hat{\delta}(t) = \delta_{tt'}/\Delta t$, where $\delta_{tt'}$ is the Kronecker delta. This leads to the following update scheme

$$x(t + \Delta t) \approx x(t) + \Delta t f(x(t)) + \sqrt{\Delta t}\eta(t), \tag{3.36}$$

with $\langle \eta(t)\eta(t') \rangle \sim \delta_{tt'}$. Note that the stochastic term now is of the order of $\sqrt{\Delta t}$, which means that the error made in each update of x will be of the order of Δt [49]. Any sequence of random numbers satisfying the correlation condition above can be used here. The easiest choice is that of Gaussian random numbers with zero mean and variance one, but if speed is of importance one may also consider to use uniformly distributed random numbers or a sum of those, giving the same second moment and mean, since these are usually much faster to generate.

Numerical integration

The simple form of the Langevin equations of motion ((3.17) and (3.18)) admits straightforward integration as they stand using the explicit forward Euler scheme described above. In the RSJ case ((3.25) and (3.29)) the situation is somewhat more complicated, partly due to the fact that the equations of motion for $\{\theta\}$ and $\mathbf{\Delta}$ are coupled and partly since the left hand side of the equations involves a summation over nearest neighbors or over all links in the system.

So far the description of the models have been completely general in terms of lattice structure, i.e., they are valid for any type of lattice. If we now for a while consider a quadratic lattice this will relieve some of the difficulties of the RSJ dynamics. On a square lattice the difference vector $\mathbf{r}_{ji}$ will only take the values $\pm\hat{\mathbf{x}}$ and $\pm\hat{\mathbf{y}}$, which means that the term $\sum_{i\in\mathcal{N}_j} \dot{A}_{ji} = \sum_{i\in\mathcal{N}_j} \dot{\mathbf{\Delta}} \cdot \mathbf{r}_{ji}$ in (3.25) is zero. In the same way, the term $\sum_{\langle ij \rangle}(\dot{\theta}_i - \dot{\theta}_j)\mathbf{r}_{ji}$ in (3.29) vanishes on a square lattice if we use periodic boundary conditions. As a consequence, the RSJ equations of motion on a square lattice with periodic boundary conditions decouple into

$$\sum_{j\in\mathcal{N}_i} \frac{\hbar}{2eR}(\dot{\theta}_i - \dot{\theta}_j) = -\sum_{j\in\mathcal{N}_i} (I_{ij}^c \sin(\theta_i - \theta_j - \mathbf{\Delta}\cdot\mathbf{r}_{ji}) + I_{ij}^n), \tag{3.37}$$

$$\frac{\hbar}{2eR}\dot{\mathbf{\Delta}} = -\bar{\mathbf{J}}^{\text{ext}} + \frac{1}{L^2}\sum_{\langle ij \rangle} (I_{ij}^c \sin(\theta_i - \theta_j - \mathbf{\Delta}\cdot\mathbf{r}_{ji}) + I_{ij}^n)\mathbf{r}_{ji}, \tag{3.38}$$

where the summation on the left hand side in the last equation has been performed and gives $\sum_{\langle ij \rangle} \dot{\mathbf{\Delta}} = L^2\dot{\mathbf{\Delta}}$, since $\mathbf{\Delta}$ is constant in space. We can further simplify these equations and put them on a Langevin type form by rewriting the left hand side of the first equation above as

$$\sum_{j\in\mathcal{N}_i} (\dot{\theta}_i - \dot{\theta}_j) = D\dot{\theta}_i, \tag{3.39}$$

where $D = -\nabla^2$ is minus the discrete analog of the Laplace operator. The corresponding matrix is defined on any lattice as

$$D_{ij} = \begin{cases} \#\text{ of neighbors to } i & \text{if } i = j \\ -1 & \text{if } j \in \mathcal{N}_i \\ 0 & \text{otherwise} \end{cases} \tag{3.40}$$

The inverse of this operator is the so called lattice Green function $G = D^{-1} = (-\nabla^2)^{-1}$. Using this we can rewrite (3.37) and (3.38) on the Langevin form

$$\frac{\hbar}{2eR}\dot{\theta}_i = -\sum_j G_{ij} \sum_{k\in\mathcal{N}_j} (I^c_{jk}\sin(\theta_j - \theta_k - \mathbf{\Delta}\cdot\mathbf{r}_{kj}) + I^n_{jk}), \tag{3.41}$$

$$\frac{\hbar}{2eR}\dot{\mathbf{\Delta}} = -\bar{\mathbf{J}}^{\text{ext}} + \frac{1}{L^2}\sum_{\langle ij\rangle}(I^c_{ij}\sin(\theta_i - \theta_j - \mathbf{\Delta}\cdot\mathbf{r}_{ji}) + I^n_{ij})\mathbf{r}_{ji}. \tag{3.42}$$

It is now possible to integrate these equations of motion using the same forward Euler scheme as in the Langevin case. Note however, that the matrix D is actually singular due to a single zero eigenvalue, and it can therefore not be inverted directly to give G. The zero eigenvalue is a consequence of the symmetry of the problem, namely that the equations of motion are invariant under a uniform rotation of all the phases. This problem can be solved by fixing one of the phases or alternatively fixing the mean of the phases and removing one row and one column from D before inverting it. In our simulations we use the condition $\sum_i \dot{\theta}_i = 0$, which physically can be interpreted as defining a reference voltage (the ground voltage) and setting it to zero.

The direct method [50, 51] of multiplying the right hand side of (3.37) with G is simple, but has the disadvantage of scaling as L^4 for a lattice of size $L \times L$. This complexity can be improved significantly to $\sim L^2\ln(L^2)$ by the use of some different methods employing fast Fourier transforms to solve the given system of equations [52, 53]. We however, make use of a fast parallel sparse matrix solver instead. With this approach, the cost in CPU time has proven to scale linearly with the number of lattice points L^2, at least up to the largest simulated system of 120×120.

Let us return to the original problem of solving the RSJ equations of motion on a general lattice. In this situation the equations will not separate or simplify and must thus be solved as they stand. A more explicit form of the (3.25) and (3.29) is

$$\sum_{j\in\mathcal{N}_i}\frac{\hbar}{2eR}(\dot{\theta}_i - \dot{\theta}_j) - (\sum_{j\in\mathcal{N}_i}\frac{\hbar}{2eR}\mathbf{r}_{ji})\cdot\dot{\mathbf{\Delta}} = -\sum_{j\in\mathcal{N}_i}(I^s_{ij} + I^n_{ij}), \tag{3.43}$$

$$\sum_i \dot{\theta}_i(\sum_{j\in\mathcal{N}_i}\frac{\hbar}{2eR}\mathbf{r}_{ji}) - (\sum_{\langle ij\rangle}\frac{\hbar}{2eR}\mathbf{r}_{ji}\mathbf{r}^T_{ji})\dot{\mathbf{\Delta}} = L^2\bar{\mathbf{J}}^{\text{ext}} - \sum_{\langle ij\rangle}(I^s_{ij} + I^n_{ij})\mathbf{r}_{ji}, \tag{3.44}$$

where we have made the substitution $\sum_{\langle ij \rangle}(\dot{\theta}_i - \dot{\theta}_j)\mathbf{r}_{ji} = \sum_i \dot{\theta}_i \sum_{j \in \mathcal{N}_i} \mathbf{r}_{ji}$ on the left hand side of the last equation. These equations are on the matrix form

$$\begin{pmatrix} D & -\lambda \\ E & -\omega \end{pmatrix} \begin{pmatrix} \dot{\theta} \\ \dot{\mathbf{\Delta}} \end{pmatrix} = \begin{pmatrix} a \\ b \end{pmatrix}. \tag{3.45}$$

For a system of size $N = L \times L$, D is the Laplacian matrix from above truncated to size $(N-1) \times (N-1)$ to remove the one singular eigenvalue, $E = \sum_{j \in \mathcal{N}_i} \mathbf{r}_{ji} = \lambda^T$ is a $2 \times (N-1)$ matrix, $\omega = \sum_{\langle ij \rangle} \mathbf{r}_{ji}\mathbf{r}_{ji}^T$ is a 2×2 matrix (leaving out the constant $\hbar/2eR$ in all expressions) and a and b the respective right hand sides of the two equations above. Once written on this form, a sparse matrix solver can be employed to efficiently solve for $\{\dot{\theta}\}$ and $\dot{\mathbf{\Delta}}$ in each update step of a forward Euler scheme.

RCSJ dynamics

The RCSJ dynamics is a generalization of the RSJ dynamics, with an added capacitance in parallel with the shunting resistance to account for charging effects in the circuit. We write the total current from site i to site j as a sum of the following contributions

$$I_{ij}^{\text{tot}} = I_{ij}^c \sin\gamma_{ij} + \frac{V_{ij}}{R} + C\dot{V}_{ij} + I_{ij}^n \equiv I_{ij}^s + I_{ij}^r + I_{ij}^C + I_{ij}^n, \tag{3.46}$$

where the voltage $V_{ij} = \frac{\hbar}{2e}\dot{\gamma}_{ij} = \frac{\hbar}{2e}(\dot{\theta}_i - \dot{\theta}_j - \dot{A}_{ij})$. Making the same transformation to dimensionless time and temperature as in the RSJ case

$$t \to t\frac{2eRI^c}{\hbar} \quad \text{and} \quad T \to T\frac{2ek_B}{\hbar I^c}, \tag{3.47}$$

gives the following simple expression for the total current

$$I_{ij}^{\text{tot}} = I_{ij}^c \sin\gamma_{ij} + \dot{\gamma}_{ij} + Q^2\ddot{\gamma}_{ij} + I^n = I_{ij}^s + I_{ij}^r + I_{ij}^C + I_{ij}^n, \tag{3.48}$$

where $Q^2 = 2eR^2I^cC/\hbar$ is a dimensionless parameter, which is simply the ratio between the two times scales RC and $\hbar/RI^c$ in the model. The parameter Q sets the amount of damping in the system. For $Q >> 1$ the time scale RC is the larger one, i.e., we have a large capacitance C and the system is strongly underdamped. The opposite limit, $Q << 1$ corresponds to a heavily overdamped system where the capacitance C is small, which is close to an RSJ model, where naturally C is zero.

The equations of motion for the phases $\{\theta\}$ and the twists $\mathbf{\Delta}$ are obtained from local current conservation and from fixing the average current in the system

$$\sum_{j \in \mathcal{N}_i} I_{ij}^{\text{tot}} = 0, \tag{3.49}$$

$$\sum_{\langle ij \rangle} I_{ij}^{\text{tot}} \mathbf{r}_{ji} = L^2 \bar{\mathbf{J}}^{\text{ext}}. \tag{3.50}$$

These equations can be written more explicitly as

$$\sum_{j\in\mathcal{N}_i}(\ddot{\theta}_i-\ddot{\theta}_j)-(\sum_{j\in\mathcal{N}_i}\mathbf{r}_{ji})\cdot\ddot{\mathbf{\Delta}}=-\frac{1}{Q^2}\sum_{j\in\mathcal{N}_i}(I^s_{ij}+I^r_{ij}+I^n_{ij}), \tag{3.51}$$

$$\sum_{\langle ij\rangle}(\ddot{\theta}_i-\ddot{\theta}_j)\mathbf{r}_{ji}-(\sum_{\langle ij\rangle}\mathbf{r}_{ji}\mathbf{r}^T_{ji})\ddot{\mathbf{\Delta}}=\frac{L^2}{Q^2}\bar{\mathbf{J}}^{\text{ext}}-\frac{1}{Q^2}\sum_{\langle ij\rangle}(I^s_{ij}+I^r_{ij}+I^n_{ij})\mathbf{r}_{ji}. \tag{3.52}$$

This system of equations is very similar to that of RSJ dynamics, except that it is second order in time. But by simply making the substitution

$$v_\theta=\dot{\theta},\quad \mathbf{v}_\Delta=\dot{\mathbf{\Delta}}, \tag{3.53}$$

we can transform to two sets of first order differential equations instead. The one containing time derivatives of v_θ and $\mathbf{v}_\Delta$ are on the same form as in the RSJ case (but with a somewhat different right hand side)

$$\begin{pmatrix}D & -\lambda\\ E & -\omega\end{pmatrix}\begin{pmatrix}\dot{\mathbf{v}}_\theta\\ \dot{\mathbf{v}}_\Delta\end{pmatrix}=\begin{pmatrix}a\\ b\end{pmatrix}. \tag{3.54}$$

Discretization of RCSJ dynamics

The RCSJ equations of motion given by (3.53) and (3.54) are most conveniently solved using a leap-frog type algorithm. This means defining the variables v_θ only on half integer time steps and the variables θ on integer time steps (and the same for the twist variables). This scheme has the advantage of being fully symmetric as well as easy to code, since both types of variables can be updated in one go. In the leap-frog discretization the "velocity" time derivative is fully symmetric and the "velocity" at time t is just the average of the velocities at the two adjacent time steps

$$\dot{v}(t)=\frac{1}{\Delta t}(v(t+\Delta t)-v(t-\Delta t)), \tag{3.55}$$

$$v(t)=\frac{1}{2}(v(t+\Delta t)+v(t-\Delta t)). \tag{3.56}$$

Inserting this in the equations of motion (3.54) leads after some simple algebra to the following matrix equation for v_θ and $\mathbf{v}_\Delta$

$$\begin{pmatrix}D & -\lambda\\ E & -\omega\end{pmatrix}\begin{pmatrix}\frac{a}{d}\mathbf{v}_\theta(t+\frac{\Delta t}{2})+\frac{b}{d}\mathbf{v}_\theta(t-\frac{\Delta t}{2})\\ \frac{a}{d}\mathbf{v}_\Delta(t+\frac{\Delta t}{2})+\frac{b}{d}\mathbf{v}_\Delta(t-\frac{\Delta t}{2})\end{pmatrix}=\frac{1}{Q^2}\begin{pmatrix}A\\ B\end{pmatrix}, \tag{3.57}$$

where the right hand side is given by $A_i=-\sum_{j\in\mathcal{N}_i}(I^s_{ij}+I^n_{ij})$ and $\mathbf{B}=L^2\bar{\mathbf{J}}^{\text{ext}}-\sum_{\langle ij\rangle}(I^s_{ij}+I^n_{ij})\mathbf{r}_{ji}$ and the constants a, b and d are defined as

$$a=2Q^2+\Delta t,\quad b=-2Q^2+\Delta t,\quad d=2Q^2\Delta t. \tag{3.58}$$

By solving (3.57) we get the new v_θ and $\mathbf{v}_\Delta$ at time $t + \Delta t/2$, which can then be used to update θ and $\mathbf{\Delta}$ at time $t + \Delta t$. This is the beauty of the simple leap-frog scheme. Another advantage of the method is that the heat current is naturally symmetric around time t. As noted in Paper II, an asymmetric discretization might cause a problem, namely that the thermal conductivity κ obtained from the Kubo formula is not consistent with the heat current response to a temperature gradient.

Note also that from (3.58) we see that if we set the time step $\Delta t = 2Q^2$, the constant b is zero and the RCSJ dynamics become fully overdamped, which actually reduces the symmetric leap-frog discretization of the RCSJ model to an asymmetric forward Euler of the RSJ equations of motion.

Chapter 4

Results: Transport in granular superconductors

This chapter is intended to serve as an introduction to Paper I and II. It includes a brief review of the Nernst effect and a summary of the important results in the papers.

4.1 Nernst and Ettingshausen effect

Starting from a completely general description of thermoelectric phenomena, we know from Chapter 1 that, assuming a weak enough applied electric field and temperature gradient, we have the following linear response relations for the electric current density $\mathbf{J}$ and the heat current density $\mathbf{J}^Q$

$$\begin{pmatrix} \mathbf{J} \\ \mathbf{J}^Q \end{pmatrix} = \begin{pmatrix} \sigma & \alpha \\ \tilde{\alpha} & \tilde{\kappa} \end{pmatrix} \begin{pmatrix} \mathbf{E} \\ -\nabla T \end{pmatrix}. \tag{4.1}$$

This defines all the thermoelectric transport coefficients including the usual electric conductivity and heat conductivity tensors σ and $\tilde{\kappa}$. The thermoelectric tensors are related by the relation $\tilde{\alpha} = \alpha T$, as a direct consequence of the Onsager relation (2.46).

There exists a number of different thermoelectric and thermomagnetic effects, all named after long-bearded fellows from past centuries, such as Seebeck, Hall, Thomson, Peltier, Righi-Leduc and a few others (see e.g. reference [54] for a review). One of these effects, which we study here, is the Nernst effect. The Nernst effect is the appearance of an electric field (in open circuit conditions) in a conductor in presence of an applied temperature gradient and an external transverse magnetic field. This electric field is perpendicular to both the temperature gradient and the

magnetic field. The Nernst coefficient ν and the Nernst signal e_N are defined as

$$\nu = \frac{e_N}{B} = \frac{1}{B}\frac{E_y}{(-\nabla_x T)}, \tag{4.2}$$

in a two dimensional geometry, where the electric field E_y, is generated by a temperature gradient $\nabla_x T$ and a transverse magnetic field B. In experiments the electric field E_y is measured in a situation with no electric transport currents present. Setting $\mathbf{J} = 0$ in (4.1) we get $\mathbf{E} = \sigma^{-1}\alpha\nabla T$. Further assuming a temperature gradient only in the x-direction ($\nabla_y T = 0$) one obtains the Nernst signal e_N in terms of the other transport coefficients as

$$e_N = \frac{\alpha_{xy}\sigma_{xx} - \alpha_{xx}\sigma_{xy}}{\sigma_{xx}^2 + \sigma_{xy}^2}. \tag{4.3}$$

To reach this result it is also necessary to use the anti-symmetric properties of the thermoelectric and electric conductivity tensors in a magnetic field, $\alpha_{xy}(\mathbf{B}) = -\alpha_{yx}(\mathbf{B})$ and $\sigma_{xy}(\mathbf{B}) = -\sigma_{yx}(\mathbf{B})$, rooted in the symmetry of the Lorentz force $\mathbf{v} \times \mathbf{B}$.

In ordinary metals the Nernst effect can be described terms of charge carriers diffusing down the temperature gradient. These charge carriers are deflected towards the edges of the sample due the Lorentz force they feel in the transverse magnetic field, and in open circuit conditions this accumulation of charge generates an electric field. However, in metals the effect is usually very small, since the two terms in the numerator of (4.3) largely cancel each other. This can also be viewed as the cancellation of two opposing currents $\sigma_{yx}E_y$ and $\alpha_{yx}(-\nabla_x T)$ (see Fig. 4.1) and is sometimes referred to as Sondheimer cancellation in the literature [12]. There are of course exceptions, for example bismuth (Bi), a semi-metal where the Nernst

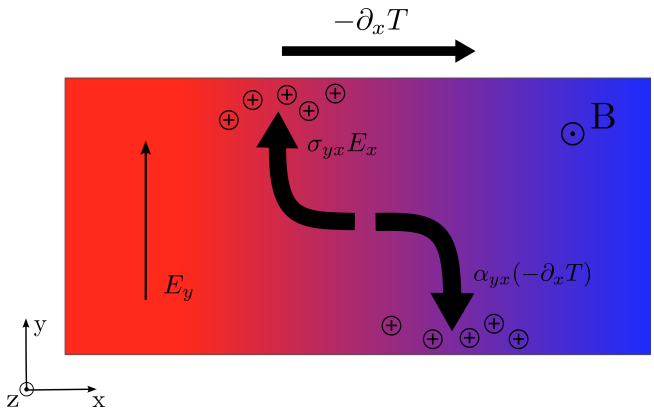

Figure 4.1: Geometry of the Nernst effect with the two opposing currents, which often cancel to give a very small Nernst effect in most ordinary metals.

effect is so large that it could be detected using late 19th century equipment by its original discoverers Nernst and Ettingshausen [55].

Let me also mention the effect dual to the Nernst effect, the Ettingshausen effect. It describes the generation of a temperature gradient in a conductor placed in transverse magnetic field when an electric current is run through it. With the same geometry as for the Nernst effect, the Ettingshausen coefficient can be defined as

$$\mathcal{E} = \frac{1}{B}\frac{(-\nabla_x T)}{J_y}. \tag{4.4}$$

Being dual, the effects are related as a consequence of the Onsager relation (2.46). The connection reads

$$\nu = \frac{1}{T}\kappa\mathcal{E}, \tag{4.5}$$

where κ is the thermal conductivity in the direction of the temperature gradient (in this case the x-direction) measured under the same conditions as the Nernst coefficient. This particular relation was found by Bridgman [56] in 1924, and is thus known as Bridgman's relation, but is really just a special case of an Onsager relation. The obvious point here is that using the relation (4.5) makes it possible to obtain the Nernst coefficient ν in an experimental situation different from the standard Nernst setup. One can simply apply a small electric current J_y and then measure the heat current response in the transverse direction $J_x^Q = \kappa(-\nabla_x T)$. Taking the ratio of these two quantities and dividing by the temperature T then gives e_N.

Vortex Nernst effect

In the vortex liquid phase of type-II superconductors the totally dominating contribution to the Nernst signal comes from mobile vortices. In the simplest possible description, the vortices move under the influence of a thermal force $\mathbf{F_t} = S_\phi(-\nabla T)$ per unit length of a single vortex line, S_ϕ being the entropy transported per unit length such a vortex line. A vortex also feels the friction force $\mathbf{F_f} = -\eta\mathbf{v}$, where η is a viscosity coefficient, and balancing these two forces gives the steady state average vortex velocity $\mathbf{v} = S_\phi(-\nabla T)/\eta$. Josephson [32] showed that the vortices generate an electric field transverse to their motion

$$\mathbf{E} = -\mathbf{v} \times \mathbf{B}, \tag{4.6}$$

which can be detected as the Nernst signal $e_N = E_y/(-\nabla_x T)$. From a similar analysis in Chapter 1, we know that the resistivity due to the motion of vortices can be written as $\rho = B\Phi_0/\eta$, where $\Phi_0 = h/2e$ is the superconducting flux quantum. Combining this with the equation for the average vortex velocity $v_x = S_\phi(-\nabla_x T)/\eta$ and the generated electric field in the y-direction $E_y = v_x B_z$ from above, gives the relation

$$e_N = \frac{S_\phi B}{\eta} = \frac{S_\phi \rho}{\Phi_0}, \tag{4.7}$$

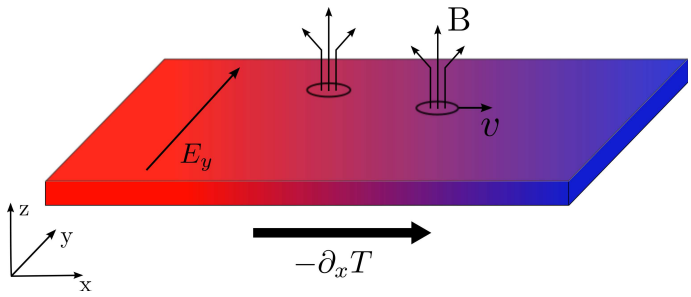

Figure 4.2: In the vortex liquid phase of type-II superconductors the electric field measured in the Nernst experiment is generated by diffusion of vortices in the transverse direction, down an applied temperature gradient.

from which one can extract the transported entropy per unit length of a vortex line S_ϕ, by measuring the Nernst signal e_N and the flux flow resistivity ρ.

An alternative, but equivalent point of view is that as a vortex moves down the temperature gradient, it induces a phase difference between the edges of the sample (this is called phase slippage) transverse to its motion, because of the phase singularity of its core, as noted by Anderson [57]. From the second Josephson equation (2.21), we then see that a voltage proportional to the time derivative of such a phase difference is generated across the sample. This is the Nernst voltage.

4.2 Anomalous vortex Nernst effect in granular superconductors

Historically the definition of the Nernst coefficient ν has differed up to a minus sign. Even authors trying to clear up the puzzlement, have seemingly just added to the confusion [58] with somewhat unclear notation. We have in (4.2) chosen the definition most commonly used in the recent literature [12, 43, 13] on the subject. Vortices moving down a temperature gradient in the x-direction generate an electric field $E_y = v_x B_z$ according to (4.6), and using our definition of the Nernst coefficient $\nu = E_y/(-\nabla_x T)B_z$, this leads to

$$v_x = \nu(-\nabla_x T). \tag{4.8}$$

Using the vortex language, the Nernst coefficient can in other words be viewed as a diagonal response of the vortex velocity to an applied temperature gradient, in contrast to the general description, where it is by definition off-diagonal. It is therefore not surprising that the (diagonal) vortex contribution usually is much larger than the (off-diagonal) charge carrier ditto. Note also that (4.8) implies that the Nernst coefficient ν is positive for vortices moving in the direction of $-\nabla_x T$, i.e., from the hotter to colder side of the sample (see Fig. 4.2). We can reformulate this statement by considering the Bridgman-Onsager relation 4.5, that gives the

heat current density in the x-direction as $J_x^Q = T\nu B_z J_y^e$. Again using $E_y = v_x B_z$ leads to

$$J_x^Q = T\nu\sigma B_z^2 v_x. \tag{4.9}$$

This means that for a positive value of ν, heat transport is always in the same direction as vortex motion. However, in Paper I we show that the Nernst coefficient ν can in fact under certain conditions become negative, implying a heat flow in the direction opposite of vortex motion. This happens in our model of granular superconductors close to certain magnetic field strengths, where the vortex lattice is particularly rigid towards thermal fluctuations, due to commensurability effects with the underlying lattice structure. In such situations the defect lattice is pron to melt at a lower temperatures [59] than the vortex lattice, resulting in mobile vortex holes diffusing down the applied temperature gradient while the vortices are pinned, thus producing a net vortex current in the opposite direction. We also find this effect in systems with moderate geometric disorder, although in that case it is not clear whether the anomalous sign of the Nernst signal is the result of the same scenario described above, or due to remnants of the vortex-hole symmetry around half-filling found in perfectly periodic systems.

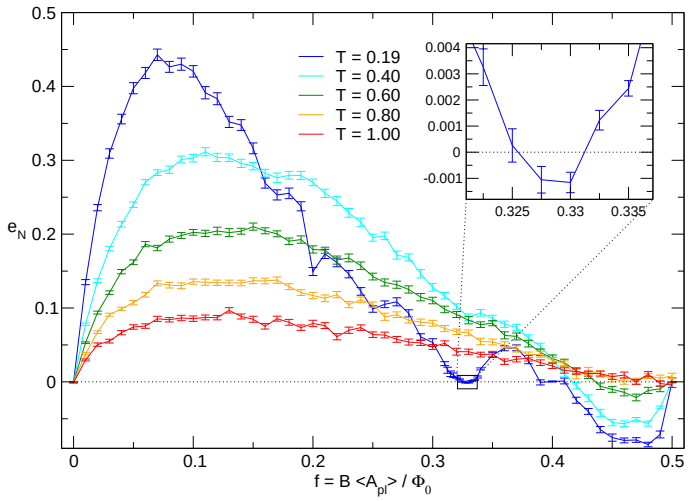

Figure 4.3: This figure from Paper I shows the Nernst signal e_N versus filling fraction f for a perfectly square lattice at different temperatures T. Note how the Nernst signal changes sign in the region just below half-filling. The inset displays a zoom-in of e_N at $T = 0.19$ around another commensurate filling $f = 1/3$, where e_N also becomes negative.

4.3 Heat current

In a theoretical description of thermoelectric phenomena the explicit form of the heat current density is crucial. Coming up with the correct expression has however turned out to be a very subtle and involved task, which has caused a lot of trouble and confusion over the years. In early investigations of thermoelectric effects in type-II superconductors in the 1960s, Caroli and Maki [60] presented a microscopic heat current expression and Schmid [61] an expression within the Ginzburg-Landau theory framework. These forms where later rectified [62, 63, 64], since they did not properly deal with the contribution to the heat current due to the magnetization of the material. This has been the key issue ever since. In more recent literature [65, 13, 14, 19, 43], the magnetic form used by Hu [63] is most commonly employed, although this has also been suggested to be (arguably) incorrect [66].

Heat current for Langevin and RCSJ dynamics

In Paper II we continue this tradition by providing two different derivations of the heat current within the framework of our models. This was done by necessity, since our main approach of calculating the Nernst signal via a Kubo formula involves forming the cross-correlation function between the electric field E_y and the transverse heat current density component J_x^Q, see (2.62). To check the validity of the final form, the resulting expression for the heat current density is tested through our simulations to obey the Onsager relation of (4.5) and in addition to give consistent results when calculating e_N and κ either from a Kubo formula or by measuring the response to an applied temperature gradient.

Derivation from continuity equations

We start from first principles and consider the differential of the total internal energy of an electromagnetic system [67]

$$de = Tds + \mathbf{H} \cdot d\mathbf{B} + \mathbf{E} \cdot d\mathbf{D} + \mu dn, \tag{4.10}$$

where e, s and n are energy, entropy and particle densities respectively. We also have the usual constitutive equations $\mathbf{B}/\mu_0 = \mathbf{H} + \mathbf{M}$ and $\mathbf{D} = \epsilon_0\mathbf{E} + \mathbf{P}$, and the Maxwell equations $\nabla \times \mathbf{B}/\mu_0 = \mathbf{J}^{\text{tot}} + \epsilon_0\dot{\mathbf{E}}$ and $\nabla \times \mathbf{H} = \mathbf{J}^{\text{tr}} + \dot{\mathbf{D}}$. The chemical potential μ is zero in our models, so the last term can be dropped here. In addition we can make use of the expression for the electromagnetic energy density

$$e = \frac{\epsilon_0\mathbf{E}^2}{2} + \frac{\mathbf{B}^2}{2\mu_0}. \tag{4.11}$$

Using these two equations together, we can find the time derivative of the heat density

$$\dot{q} = T\dot{s} = -\nabla \cdot (\mathbf{E} \times \mathbf{M}) - \mathbf{E} \cdot (\mathbf{J}^{\text{tot}} - \mathbf{J}^{\text{tr}}). \tag{4.12}$$

This in on a form of a continuity equation and we can immediately identify the heat current density as $\mathbf{J}^Q = \mathbf{E} \times \mathbf{M}$. But since we do not use the magnetization density $\mathbf{M}$ in our simulations, we want to find a way to rewrite it in terms of currents. Furthermore we want the heat current in say the x-direction. To this end, multiply the above continuity equation for the heat current density with x, integrate over the system, and use that in a stationary state $\dot{q} = 0$. Assuming open boundary conditions for convenience, we obtain after a few lines of algebra that the average heat current density in the x-direction is given by

$$\bar{J}_x^Q = \frac{1}{\Omega} \int \phi (J_x^{\text{tot}} - J_x^{\text{tr}}) d\Omega + \frac{1}{\Omega} \int x(-\dot{\mathbf{A}}) \cdot (\mathbf{J}^{\text{tot}} - \mathbf{J}^{\text{tr}}) d\Omega. \tag{4.13}$$

We have here two contributions. The first one is local and can be obtained on a explicitly discrete form in another fashion by forming a continuity equation for the energy in the particular model we consider. For both Langevin and RCSJ dynamics, such a calculation gives

$$\sum_{\langle ij \rangle} \frac{1}{2} (V_i + V_j)(I_{ij} - I_{ij}^{\text{tr}}), \tag{4.14}$$

where I_{ij} denotes the supercurrent I_{ij}^s for Langevin dynamics and the full current I_{ij}^{tot} in the RCSJ case. The second term is in our model non-local, since $\dot{\mathbf{A}} = \frac{\Phi_0}{2\pi} \mathbf{\Delta}$ is spatially uniform and thus can not be captured by considering a continuity equation for the local energy density. Rewriting this term on a discrete form we get the total average heat current density in the x-direction as

$$\bar{J}_{\text{tot},x}^Q = \frac{1}{L_x L_y} \sum_{\langle ij \rangle} \left(\frac{1}{2} x_{ji} (V_i + V_j) - x_{ij}^c \dot{A}_{ij} \right) (I_{ij} - I_{ij}^{\text{tr}}). \tag{4.15}$$

which is the actual expression we use in the simulations and what goes into the Kubo formula to calculate the Nernst signal and thermal conductivity.

Derivation using functional integrals

The starting point of the second derivation is the Kubo formula giving the Nernst signal as

$$e_N = \frac{\Omega}{2k_B T^2} \int_{-\infty}^{\infty} \langle E_y(t) J_x^Q(0) \rangle dt. \tag{4.16}$$

This equation can be used to identify the heat current density J_x^Q, provided that we can find another way of deriving the Nernst response for the specific models we use and then compare the two expressions. This is possible by reformulating the problem using functional field integral methods.

In the functional integral language an ensemble average of a dynamical variable $A(t)$ is given by

$$\langle A(t)\rangle = \frac{1}{Z}\int [dx]A[x(t)]e^{-S[x]}J[x], \tag{4.17}$$

where $e^{-S[x]}$ is the statistical weight of a given realization of the stochastic process $x(t)$ and $[dx]$ is the appropriate integral measure. This can be derived considering a general Langevin equation

$$\dot{\mathbf{x}}(t) = \mathbf{f}[\mathbf{x}(t)] + \boldsymbol{\eta}(t), \tag{4.18}$$

with additive Gaussian white noise $\langle \eta_i(t)\eta_j(t')\rangle = 2D\delta_{ij}\delta(t-t')$. From a standard path integral formulation of the Gaussian probability distribution of $\boldsymbol{\eta}$ (see e.g. [68] for a review) an ensemble average is defined as a functional integration over the noise

$$\langle A(t)\rangle = \int [d\eta]A[\boldsymbol{\eta}(t)]e^{-S[\boldsymbol{\eta}]}, \quad S = \frac{1}{4D}\int \boldsymbol{\eta}(t)^2 dt. \tag{4.19}$$

The trick now is to use the functional integral identity

$$\mathbf{1} = \int [dx]\delta[x - x_{\mathrm{sol}}] = \int [dx][d\tilde{x}]e^{i(\dot{\mathbf{x}}-\mathbf{f}-\boldsymbol{\eta})\cdot\tilde{\mathbf{x}}}, \tag{4.20}$$

where the delta functional $\delta[x - x_{\mathrm{sol}}]$ enforces $\mathbf{x}$ to solve the Langevin equation (4.18). Inserting (4.20) in (4.19) and performing the functional integrals over $\boldsymbol{\eta}$ and $\tilde{\mathbf{x}}$ one obtains the form corresponding to (4.17) with an integration going only over $\mathbf{x}$

$$\langle A(t)\rangle \sim \int [dx]A[x(t)]e^{-S[x]}J[x], \quad S[x] = \frac{1}{4D}\int (\dot{\mathbf{x}}(t) - \mathbf{f}(t))^2 dt. \tag{4.21}$$

Here $J[x]$ is a constant from the functional integrations over $\boldsymbol{\eta}$ and $\tilde{\mathbf{x}}$, or equivalently a Jacobian stemming from the change of integration variables from $\boldsymbol{\eta}$ to $\mathbf{x}$.

Returning to the task of finding the heat current, we remember the definition of the Nernst signal as the response of the electric field E_y to an applied temperature gradient in the x-direction. Defining the gradient T' (which is assumed to be small) through the spatially varying temperature $T(x) = T_0 - T'x$, we then have $e_N = \delta\langle E_y\rangle/\delta T'$. Since the temperature dependence sits only in the action S, the response of E_y to a static T' in steady state is simply

$$\frac{\delta\langle E_y\rangle}{\delta T'} = \int_{-\infty}^{\infty}\langle E_y(t)Q(0)\rangle dt, \quad Q(0) = -\frac{\delta S[\theta]}{\delta T'}\bigg|_{T'=0}. \tag{4.22}$$

Looking at (4.16) makes it tempting to identify $Q(t)$ with $J_x^Q/2k_BT^2$, but this is not quite true since $J_x^Q(t)$ is odd under time reversal and $Q(t)$ consists of both an odd and an even part. We must therefore first separate out the odd part of $Q(t)$ to make the identification with the heat current density. Now, given the equations

of motion for Langevin and RCSJ dynamics we can write down an expression for the dynamical action S (as described above), which enables us to identify the heat current density for the respective model. What pops out in the end is precisely the same as in the first derivation, namely the expression in (4.15). Note that what we do in this second approach is essentially to derive a Kubo formula for the Nernst signal e_N valid for the models we employ. Since we know the structure of the Kubo formula, the form the heat current density can also be identified.

4.4 Transport coefficients in weak and zero magnetic fields

Zero field thermal conductivity in RCSJ dynamics

Having derived an expression for the heat current also enables us to calculate the thermal conductivity κ. In Paper II we perform a quite careful analysis of κ in zero magnetic field for RCSJ dynamics on a square lattice. At low temperatures we assume that fluctuations are small so that we can linearize the RCSJ equations of motion ((3.49) and (3.50)). In this limit it turns out that κ is divergent with system size L. The most divergent contribution to κ is

$$\frac{k_B}{RC}\left(\frac{1}{4\pi}\ln\frac{L}{a}+\frac{1}{\Omega}\frac{L_x^2-1}{12}\right). \tag{4.23}$$

Note that this expression is divergent not only in the $L\to\infty$ limit, but also for $C\to 0$, which corresponds to RSJ dynamics (completely overdamped RCSJ dynamics). In our simulations we in many cases subtract this temperature independent

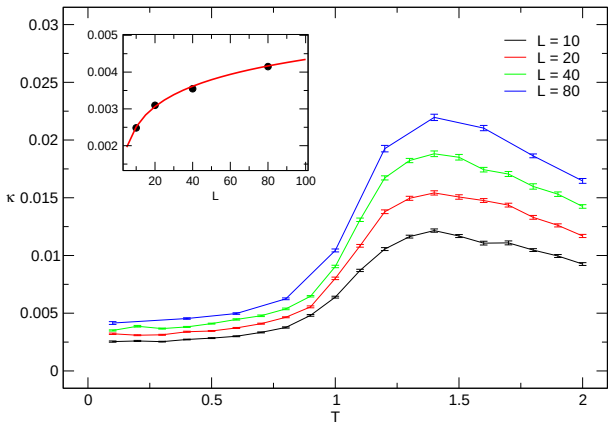

Figure 4.4: Heat conductivity κ versus temperature T in zero magnetic field for square lattices of different sizes L with RCSJ dynamics ($Q = 10$). The inset shows the divergence with system size L at low T. The circles are simulation data and the smooth red curve is the analytic result obtained from a linearized model.

divergent background, since we have already calculated it analytically and the subtraction reduces the noise in the sampled data. This is especially useful in the case of RSJ dynamics where the divergent contribution is proportional to $1/\Delta t$, where Δt is the time step of the discretization.

Fig. 4.4 displays a plot of κ versus temperature T at zero magnetic field for RCSJ dynamics on square lattices of different sizes (without the previously mentioned subtraction). The divergence with system size at low temperatures is shown in the inset. The simulation data (black dots) follow very well the logarithmic divergence seen in the analytic result (red curve) of (4.23). Apart from the divergence at low temperature, which is constant in temperature, there is an additional divergence seen at all finite T in the big plot of Fig. 4.4. The form of the divergence can be verified to be $\sim \ln(L/a)$, with $a = 0.7$, over the entire temperature range except close to $T_{\mathrm{BKT}} \simeq 0.9$. The origin of this second divergence with system size is not clear to us, but is seems only to be present a zero magnetic field for RCSJ (and RSJ) dynamics. For Langevin dynamics κ shows no signs of any type of divergence.

Weak magnetic fields

The sign reversal of the Nernst effect seen in Fig. 4.3 is an effect due to geometric frustration happening at relatively high magnetic fields. Such an effect can only be expected to be seen in superconductors with some sort of granular structure. However, at lower field strengths, where the typical vortex separation is much larger than the lattice constant $a \sim \xi_0$ frustration effects are absent, and the model we use should in principle also be applicable as description of continuous two-dimensional (and quasi-two dimensional) type-II superconductors. The Nernst signal e_N versus temperature for low fields from our simulations indeed show a qualitatively

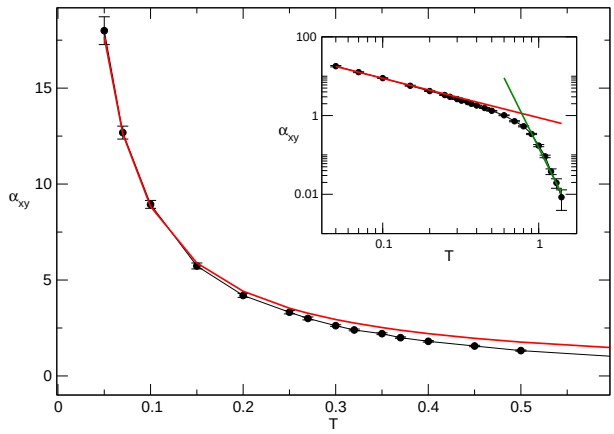

Figure 4.5: The off-diagonal component of the thermoelectric tensor α_{xy} versus temperature T for Langevin dynamics on a square 20×20 lattice at filling $f = 0.01$.

similar shape to the tilted hill profile observed in experiments on cuprates and ordinary type-II superconductors [12, 8]. Another interesting observation is the behavior of the off-diagonal component of the thermoelectric tensor α_{xy}. For the models we employ there is no Hall effect, i.e, $\sigma_{xy} = 0$. From (4.3) we then have $e_N = \alpha_{xy}/\sigma_{xx} = \alpha_{xy}\rho_{xx}$ (note also that α_{xy} is proportional to the vortex transport entropy through (4.7)). According to theoretical calculations of Gaussian fluctuations of the amplitude of the superconducting order parameter [17] α_{xy} should fall of as $\sim 1/(T - T_c)$ for weak magnetic fields in two dimensions. Some experiments [16, 69] on thin-film superconductors also seem to support this prediction. In Fig. 4.5 α_{xy} from our simulations is plotted a function of temperature, along with a fit to the $1/T$-law (red curve) (in our models $T_c = 0$ in a finite weak magnetic field). Considering that our model only takes into account phase fluctuations and keeps the amplitude of the order parameter constant, it is quite unexpected to see such a good fit. As can be seen in the inset, α_{xy} definitely goes as $\sim 1/T$ at low T, but falls of much faster, somewhere close to $1/T^8$, in the high temperature limit. This goes against the results of a simulation study also considering a phase only model [19], where a $\sim 1/T^4$ dependence of α_{xy} in the high temperature region was found.

Chapter 5

Summary and conclusions

In the first part of this thesis, some general theory regarding superconductivity and non-equilibrium thermodynamics is briefly reviewed. We introduce a model for two-dimensional granular superconducting systems within a phase only description employing Langevin or RCSJ dynamics. The model formulation is valid for any type of lattice structure.

In Paper I we study the Nernst effect due to vortex motion through numerical simulations of this model. We find as our main result that the Nernst signal e_N, around certain magnetic fields, displays an anomalous sign change, corresponding to a reversal of the net vortex flow, from colder to hotter. The effect is seen for both Langevin and RSJ dynamics in regular lattices as well as in lattices with moderate geometric disorder. For irregular arrays the sign reversal might however have somewhat different origin than in the regular case, but should nevertheless be possible to observe in experiments on artificial Josephson junction arrays and thin-film granular superconductors.

Paper II is a continuation of Paper I in the sense that the Nernst effect and related transport phenomena such as the diagonal thermal conductivity κ and electrical resistivity ρ are studied within the framework of our previously defined models. The rather subtle expression for the heat current density is derived in two separate ways for Langevin and RCSJ dynamics. We also observe that a proper *symmetric* discretization has to be used for this heat current expression, in order to obtain self-consistent results for κ. Further, analytical calculations show that the thermal conductivity at low temperatures for RCSJ dynamics has a divergent contribution which is temperature independent. Subtracting this background still leaves κ logarithmically divergent with the system size L. The origin of this second divergence is at this time unknown to us and requires further investigation.

Finally, the off-diagonal component of the thermoelectric tensor α_{xy}, obtained from our simulations as e_N/ρ, is observed to display a $\sim 1/T$ dependence at low T, something which is also predicted by a theory considering Gaussian fluctuations of the superconducting order parameter, and consistent with experiments on thin-

film superconductors, both of cuprate and ordinary type. The agreement is quite intriguing due to the apparent difference of the models, and also means that this feature of α_{xy} can not be used to discriminate between the two scenarios.

Bibliography

[1] A. Andersson and J. Lidmar, "Anomalous Nernst effect and heat transport by vortex vacancies in granular superconductors," *Phys. Rev. B*, vol. 81, p. 060508, Feb 2010.

[2] A. Andersson and J. Lidmar, "Heat transport and thermoelectric effects in granular superconductors," 2010.

[3] P. R. Solomon and F. A. Otter, "Thermomagnetic Effects in Superconductors," *Phys. Rev.*, vol. 164, pp. 608–618, Dec 1967.

[4] R. P. Huebener and A. Seher, "Nernst Effect and Flux Flow in Superconductors. I. Niobium," *Phys. Rev.*, vol. 181, pp. 701–709, May 1969.

[5] R. P. Huebener and A. Seher, "Nernst Effect and Flux Flow in Superconductors. II. Lead Films," *Phys. Rev.*, vol. 181, pp. 710–716, May 1969.

[6] T. T. M. Palstra, B. Batlogg, L. F. Schneemeyer, and J. V. Waszczak, "Transport entropy of vortex motion in $YBa_2Cu_3O_7$," *Phys. Rev. Lett.*, vol. 64, pp. 3090–3093, Jun 1990.

[7] S. J. Hagen, C. J. Lobb, R. L. Greene, M. G. Forrester, and J. Talvacchio, "Flux-flow Nernst effect in epitaxial $YBa_2Cu_3O_7$," *Phys. Rev. B*, vol. 42, pp. 6777–6780, Oct 1990.

[8] H.-C. Ri, R. Gross, F. Gollnik, A. Beck, R. P. Huebener, P. Wagner, and H. Adrian, "Nernst, Seebeck, and Hall effects in the mixed state of $YBa_2Cu_3O_{7-\delta}$ and $Bi_2Sr_2CaCu_2O_{8+x}$ thin films: A comparative study," *Phys. Rev. B*, vol. 50, pp. 3312–3329, Aug 1994.

[9] Z. A. Xu, N. P. Ong, Y. Wang, T. Kakeshita, and S. Uchida, "Vortex-like excitations and the onset of superconducting phase fluctuation in underdoped $La_{2-x}Sr_xCuO_4$," *Nature*, vol. 406, pp. 486–488, Aug 2000.

[10] Y. Wang, Z. A. Xu, T. Kakeshita, S. Uchida, S. Ono, Y. Ando, and N. P. Ong, "Onset of the vortexlike Nernst signal above T_c in $La_{2-x}Sr_xCuO_4$ and $Bi_2Sr_{2-y}La_yCuO_6$," *Phys. Rev. B*, vol. 64, p. 224519, Nov 2001.

[11] Y. Wang, N. P. Ong, Z. A. Xu, T. Kakeshita, S. Uchida, D. A. Bonn, R. Liang, and W. N. Hardy, "High Field Phase Diagram of Cuprates Derived from the Nernst Effect," *Phys. Rev. Lett.*, vol. 88, p. 257003, Jun 2002.

[12] Y. Wang, L. Li, and N. P. Ong, "Nernst effect in high-T_c superconductors," *Phys. Rev. B (Condensed Matter and Materials Physics)*, vol. 73, no. 2, p. 024510, 2006.

[13] I. Ussishkin, S. L. Sondhi, and D. A. Huse, "Gaussian Superconducting Fluctuations, Thermal Transport, and the Nernst Effect," *Phys. Rev. Lett.*, vol. 89, p. 287001, Dec 2002.

[14] S. Mukerjee and D. A. Huse, "Nernst effect in the vortex-liquid regime of a type-II superconductor," *Phys. Rev. B*, vol. 70, p. 014506, Jul 2004.

[15] A. Pourret, H. Aubin, J. Lesueur, C. A. Marrache-Kikuchi, L. Berge, L. Dumoulin, and K. Behnia, "Observation of the Nernst signal generated by fluctuating Cooper pairs," *Nature Physics*, vol. 2, no. 10, pp. 683–686, 2006.

[16] A. Pourret, H. Aubin, J. Lesueur, C. A. Marrache-Kikuchi, L. Bergé, L. Dumoulin, and K. Behnia, "Length scale for the superconducting Nernst signal above T_c in $Nb_{0.15}Si_{0.85}$," *Phys. Rev. B*, vol. 76, p. 214504, Dec 2007.

[17] I. Ussishkin, "Superconducting fluctuations and the Nernst effect: A diagrammatic approach," *Phys. Rev. B*, vol. 68, p. 024517, Jul 2003.

[18] M. N. Serbyn and M. A. Skvortsov and A. A. Varlamov and Victor Galitski, "Giant nernst effect due to fluctuating cooper pairs in superconductors," *Phys. Rev. Lett.*, vol. 102, no. 6, p. 067001, 2009.

[19] D. Podolsky, S. Raghu, and A. Vishwanath, "Nernst Effect and Diamagnetism in Phase Fluctuating Superconductors," *Phys. Rev. Lett.*, vol. 99, no. 11, p. 117004, 2007.

[20] S. A. Hartnoll, P. K. Kovtun, M. Müller, and S. Sachdev, "Theory of the Nernst effect near quantum phase transitions in condensed matter and in dyonic black holes," *Phys. Rev. B*, vol. 76, no. 14, p. 144502, 2007.

[21] A. Hackl, M. Vojta, and S. Sachdev, "Quasiparticle Nernst effect in stripe-ordered cuprates," *Phys. Rev. B*, vol. 81, p. 045102, Jan 2010.

[22] L. Li, Y. Wang, S. Komiya, S. Ono, Y. Ando, G. D. Gu, and N. P. Ong, "Diamagnetism and Cooper pairing above T_c in cuprates," *Phys. Rev. B*, vol. 81, p. 054510, Feb 2010.

[23] J. Bardeen, L. N. Cooper, and J. R. Schrieffer, "Theory of Superconductivity," *Phys. Rev.*, vol. 108, pp. 1175–1204, Dec 1957.

[24] V. L. Ginzburg and L. D. Landau *Zh. Eksp. Teor. Fiz.*, vol. 20, no. 1064, 1950.

[25] A. J. Leggett, *Quantum Liquids: Bose Condensation and Cooper Pairing in Condensensed-Matter Systems*. Oxford University Press, Oxford, 2006.

[26] A. A. Gor'kov *Zh. Eksp. Teor. Fiz.*, vol. 36, no. 1918, 1959.

[27] L. P. Pitaevskii, *Superconductivity: Conventional and Unconventional Superconductors*, vol. 2. Springer, Berlin, 2008.

[28] A. A. Abrikosov *Zh. Eksp. Teor. Fiz.*, vol. 32, no. 1442, 1957.

[29] W. H. Kleiner, L. M. Roth, and S. H. Autler, "Bulk Solution of Ginzburg-Landau Equations for Type II Superconductors: Upper Critical Field Region," *Phys. Rev.*, vol. 133, pp. A1226–A1227, Mar 1964.

[30] D. S. Fisher, M. P. A. Fisher, and D. A. Huse, "Thermal fluctuations, quenched disorder, phase transitions, and transport in type-II superconductors," *Phys. Rev. B*, vol. 43, pp. 130–159, Jan 1991.

[31] G. Blatter, M. V. Feigel'man, V. B. Geshkenbein, A. I. Larkin, and V. M. Vinokur, "Vortices in high-temperature superconductors," *Rev. Mod. Phys.*, vol. 66, pp. 1125–1388, Oct 1994.

[32] B. D. Josephson, "Potential differences in the mixed state of type II superconductors," *Physics Letters*, vol. 16, no. 3, pp. 242 – 243, 1965.

[33] V. Berezinkii, "Destruction of Long-range Order in One-dimensional and Two-dimensional Systems having a Continuous Symmetry Group I. Classical Systems," *Sov. Phys. JETP*, vol. 32, pp. 493–500, 1971.

[34] J. M. Kosterlitz and D. J. Thouless, "Ordering, metastability and phase transitions in two-dimensional systems," *Journal of Physics C: Solid State Physics*, vol. 6, no. 7, p. 1181, 1973.

[35] B. D. Josephson, "Possible new effects in superconductive tunnelling," *Phys. Lett.*, vol. 1, no. 7, pp. 251 – 253, 1962.

[36] R. Feynman, *The Feynman Lectures on Physics*, vol. 3. Addison-Wesley, 1963.

[37] *Physica B: Condensed Matter*, vol. 222, no. 4, pp. 253 – 406, 1996. Proceedings of the ICTP Workshop on Josephson Junction Arrays.

[38] R. Kubo, "Statistical-Mechanical Theory of Irreversible Processes. I. General Theory and Simple Applications to Magnetic and Conduction Problems," *Journal of the Physical Society of Japan*, vol. 12, no. 6, pp. 570–586, 1957.

[39] L. Onsager, "Reciprocal Relations in Irreversible Processes. I.," *Phys. Rev.*, vol. 37, pp. 405–426, Feb 1931.

[40] L. Onsager, "Reciprocal Relations in Irreversible Processes. II.," *Phys. Rev.*, vol. 38, pp. 2265–2279, Dec 1931.

[41] J. M. Luttinger, "Theory of Thermal Transport Coefficients," *Phys. Rev.*, vol. 135, pp. A1505–A1514, Sep 1964.

[42] B. J. Kim, P. Minnhagen, and P. Olsson, "Vortex dynamics for two-dimensional XY models," *Phys. Rev. B*, vol. 59, pp. 11506–11522, May 1999.

[43] A. Larkin and A. Varlamov, *Theory of Fluctuations in Superconductors*. Oxford University Press, New York, 2009.

[44] J. R. Tucker and B. I. Halperin, "Onset of Superconductivity in One-Dimensional Systems," *Phys. Rev. B*, vol. 3, pp. 3768–3782, Jun 1971.

[45] P. C. Hohenberg and B. I. Halperin, "Theory of dynamic critical phenomena," *Rev. Mod. Phys.*, vol. 49, pp. 435–479, Jul 1977.

[46] J. B. Johnson, "Thermal Agitation of Electricity in Conductors," *Phys. Rev.*, vol. 32, p. 97, Jul 1928.

[47] H. Nyquist, "Thermal Agitation of Electric Charge in Conductors," *Phys. Rev.*, vol. 32, pp. 110–113, Jul 1928.

[48] E. Granato and D. Domínguez, "Resistivity scaling and critical dynamics of fully frustrated Josephson-junction arrays with on-site dissipation," *Phys. Rev. B*, vol. 71, p. 094521, Mar 2005.

[49] M. L. Bellac, F. Mortessagne, and G. G. Batrouni, *Equilibrium and Non-equilibrium Statistical Thermodynamics*. Cambridge University Press, 2004.

[50] K. K. Mon and S. Teitel, "Phase Coherence and Nonequilibrium Behavior in Josephson Junction Arrays," *Phys. Rev. Lett.*, vol. 62, pp. 673–676, Feb 1989.

[51] J. S. Chung, K. H. Lee, and D. Stroud, "Dynamical properties of superconducting arrays," *Phys. Rev. B*, vol. 40, pp. 6570–6580, Oct 1989.

[52] H. Eikmans and J. E. van Himbergen, "Dynamic simulations of arrays of Josephson junctions," *Phys. Rev. B*, vol. 41, pp. 8927–8932, May 1990.

[53] V. I. Marconi and D. Domínguez, "Melting and transverse depinning of driven vortex lattices in the periodic pinning of Josephson junction arrays," *Phys. Rev. B*, vol. 63, p. 174509, Apr 2001.

[54] H. B. Callen, "The Application of Onsager's Reciprocal Relations to Thermoelectric, Thermomagnetic, and Galvanomagnetic Effects," *Phys. Rev.*, vol. 73, pp. 1349–1358, Jun 1948.

[55] A. V. Ettingshausen and W. H. Nernst *Wied. Ann.*, vol. 29, p. 343, 1886.

[56] P. W. Bridgman, "The Connections between the Four Transverse Galvanomagnetic and Thermomagnetic Phenomena," *Phys. Rev.*, vol. 24, pp. 644–651, Dec 1924.

[57] P. W. Anderson, "Considerations on the Flow of Superfluid Helium," *Rev. Mod. Phys.*, vol. 38, pp. 298–310, Apr 1966.

[58] K. Behnia, "The Nernst effect and the boundaries of the Fermi liquid picture," *Journal of Physics: Condensed Matter*, vol. 21, no. 11, p. 113101, 2009.

[59] M. Franz and S. Teitel, "Vortex-lattice melting in two-dimensional superconducting networks and films," *Phys. Rev. B*, vol. 51, pp. 6551–6574, Mar 1995.

[60] C. Caroli and K. Maki, "Motion of the Vortex Structure in Type-II Superconductors in High Magnetic Field," *Phys. Rev.*, vol. 164, pp. 591–607, Dec 1967.

[61] A. Schmid, "A time dependent Ginzburg-Landau equation and its application to the problem of resistivity in the mixed state," *Zeitschrift für Physik B Condensed Matter*, vol. 5, pp. 302–317, Oct 1966.

[62] K. Maki, "Thermomagnetic Effects in Dirty Type-II Superconductors," *Phys. Rev. Lett.*, vol. 21, pp. 1755–1757, Dec 1968.

[63] C.-R. Hu, "Heat-current operator and transport entropy of vortices in type-II superconductors," *Phys. Rev. B*, vol. 13, pp. 4780–4783, Jun 1976.

[64] A. T. Dorsey, "Vortex motion and the Hall effect in type-II superconductors: A time-dependent Ginzburg-Landau theory approach," *Phys. Rev. B*, vol. 46, pp. 8376–8392, Oct 1992.

[65] N. R. Cooper, B. I. Halperin, and I. M. Ruzin, "Thermoelectric response of an interacting two-dimensional electron gas in a quantizing magnetic field ," *Phys. Rev. B*, vol. 55, pp. 2344–2359, Jan 1997.

[66] A. Sergeev, M. Y. Reizer, and V. Mitin, "Heat current in the magnetic field: Nernst-Ettingshausen effect above the superconducting transition," *Phys. Rev. B*, vol. 77, p. 064501, Feb 2008.

[67] L. D. Landau and E. M. Lifshitz, *Electrodynamics of Continuous Media*, vol. 8. Pergamon Press, Oxford, 1960.

[68] H. Kleinert, *Path Integrals in Quantum Mechanics, Statistics, Polymer Physics, and Financial Markets, 3rd Edition.* World Scientific, 2004.

[69] I. Kokanović, J. R. Cooper, and M. Matusiak, "Nernst Effect Measurements of Epitaxial $Y_{0.95}Ca_{0.05}Ba_2(Cu_{1-x}Zn_x)_3O_y$ and $Y_{0.9}Ca_{0.1}Ba_2Cu_3O_y$ Superconducting Films," *Phys. Rev. Lett.*, vol. 102, p. 187002, May 2009.